Title

Comparative analyses of responses to exogenous and endogenous antiherbivore elicitors enable a forward genetics approach to identify maize gene candidates mediating sensitivity to herbivore-associated molecular patterns

Journal

The Plant Journal, 108(5)

ISSN

0960-7412

Authors

Poretsky, Elly
Ruiz, Miguel
Ahmadian, Nazanin
et al.

Publication Date

2021-12-01

DOI

10.1111/tpj.15510

Peer reviewed

the plant journal

SEB SOCIETY FOR EXPERIMENTAL BIOLOGY

The Plant Journal (2021) doi: 10.1111/tpj.15510

Comparative analyses of responses to exogenous and endogenous antiherbivore elicitors enable a forward genetics approach to identify maize gene candidates mediating sensitivity to herbivore-associated molecular patterns

Elly Poretsky[1], Miguel Ruiz[1], Nazanin Ahmadian[1], Adam D. Steinbrenner[2], Keini Dressano[1], Eric A. Schmelz[1] and Alisa Huffaker[1,*]

[1]*Division of Biology, University of California San Diego, La Jolla, CA 92093, USA, and*
[2]*Department of Biology, University of Washington, Seattle, WA 98195, USA*

Received 23 July 2021; revised 3 September 2021; accepted 7 September 2021.
*For correspondence (e-mail ahuffaker@ucsd.edu).

SUMMARY

Crop damage by herbivorous insects remains a significant contributor to annual yield reductions. Following attack, maize (*Zea mays*) responds to herbivore-associated molecular patterns (HAMPs) and damage-associated molecular patterns (DAMPs), activating dynamic direct and indirect antiherbivore defense responses. To define underlying signaling processes, comparative analyses between plant elicitor peptide (Pep) DAMPs and fatty acid–amino acid conjugate (FAC) HAMPs were conducted. RNA sequencing analysis of early transcriptional changes following Pep and FAC treatments revealed quantitative differences in the strength of response yet a high degree of qualitative similarity, providing evidence for shared signaling pathways. In further comparisons of FAC and Pep responses across diverse maize inbred lines, we identified Mo17 as part of a small subset of lines displaying selective FAC insensitivity. Genetic mapping for FAC sensitivity using the intermated B73 × Mo17 population identified a single locus on chromosome 4 associated with FAC sensitivity. Pursuit of multiple fine-mapping approaches further narrowed the locus to 19 candidate genes. The top candidate gene identified, termed *FAC SENSITIVITY ASSOCIATED* (*ZmFACS*), encodes a leucine-rich repeat receptor-like kinase (LRR-RLK) that belongs to the same family as a rice (*Oryza sativa*) receptor gene previously associated with the activation of induced responses to diverse Lepidoptera. Consistent with reduced sensitivity, *ZmFACS* expression was significantly lower in Mo17 as compared to B73. Transient heterologous expression of ZmFACS in *Nicotiana benthamiana* resulted in a significantly increased FAC-elicited response. Together, our results provide useful resources for studying early elicitor-induced antiherbivore responses in maize and approaches to discover gene candidates underlying HAMP sensitivity in grain crops.

Keywords: quantitative genetics, plant–herbivore interactions, volatiles, signaling and hormones, peptide signaling, *Zea mays*.

INTRODUCTION

Crop stress driven by insect pests and disease can cause 50% losses of total annual yield, with increased severity of environmental stresses expected to exacerbate future losses (Chakraborty and Newton, 2011). Among the more damaging insect pests are lepidoptera in the family Noctuidae, which include many *Spodoptera* species (Parra et al., 2021). For example, fall armyworm (FAW; *Spodoptera frugiperda*) is a highly polyphagous pest that attacks over 350 host plants across 76 plant families (Montezano et al., 2018). Despite success as a generalist, FAW exhibits measurable specialization on grain crops like maize (*Zea mays*), driving defoliation, seedling loss, and introduction of fungal pathogens that contaminate grain with mycotoxins (Overton et al., 2021). Together with native *Heliothis* spp. and *Helicoverpa* spp. crop pests in the Americas, FAW has been partially controlled by the transgenic approach of stacking *Bacillus thuringensis* (Bt) cytotoxin-encoding genes in many crops (Shehryar et al., 2020). However, despite robust protective Bt crop traits, evidence in

multiple countries, including Brazil, Puerto Rico, and parts of the United States, is emerging that FAW is evolving resistance to Bt-mediated crop protection (Horikoshi et al., 2016). Furthermore, FAW is a formidable global invasive pest. In 2016, FAW was detected in West Africa and has now spread across the entire continent, causing annual losses of billions of dollars (Day et al., 2017). Entering India in 2018, FAW has rapidly proliferated throughout Asia and is now found in Australia (Overton et al., 2021). Given the global challenge posed by noctuid pests and potential breakdown of current control measures, new knowledge of plant resistance mechanisms and control strategies are essential to reduce crop losses (Douglas, 2018).

As a major crop species attacked by diverse lepidoptera, including FAW and *Spodoptera exigua*, maize has been a leading research model for understanding plant responses to herbivory. For example, in what is now appreciated as a common phenomenon, indirect plant defense responses against lepidopteran pests were first described in maize (Turlings et al., 1990). The elicited production of volatile organic compounds (VOCs) emitted from leaves following *Spodoptera* herbivory can attract parasitoid wasps such as *Cotesia marginiventris*, enhance parasitization rates, and aid in plant protection (Turlings and Erb, 2018; Turlings et al., 1990). Herbivore-elicited volatiles are produced by young maize leaves, and while there is qualitative and quantitative variation among inbred lines, the blend is largely dominated by monoterpenes, homoterpenes, sesquiterpenes, fatty acid-derived green leafy volatiles (GLVs), indole, and methyl anthranilate (Degen et al., 2004). In addition to attracting parasitoids, indole and GLV components of the volatile blend act in interplant communication, priming defense responses in undamaged neighboring plants (Engelberth et al., 2004; Erb et al., 2015). Volatiles also mediate indirect maize defenses belowground; herbivory by Western corn rootworm (WCR; *Diabrotica virgifera*) larvae triggers emission of the sesquiterpene β-caryophyllene, attracting entomophagous nematodes that prey on the larvae (Rasmann et al., 2005). In addition to volatiles, maize produces complex blends of directly protective chemicals and defensive proteins that vary with tissue, developmental stage, and genetic background. Toxic and antifeedant chemicals include the insecticidal silk-localized C-glycosyl flavone maysin (Casas et al., 2016; Waiss et al., 1979), benzoxazinoid toxins such as dihydroxy-7-methoxy-1,4-benzoxazin-3-one glucoside (DIMBOA-Glc) and 2-hydroxy-4,7-dimethoxy-1,4-benzoxazin-3-one glucoside (HDMBOA-Glc) (Maag et al., 2016; Oikawa et al., 2004; Wouters et al., 2016), and antifeedant diterpenoids (Schmelz et al., 2011). While some maize defenses such as DIMBOA-Glc are constitutively present in young seedlings, the production of many defenses is upregulated by herbivory, enabling added protection against attack while minimizing production of costly defenses in the absence of herbivory (Erb, 2018; Fürstenberg-Hägg et al., 2013; Mithöfer and Boland, 2012). Inducible responses can vary across genotypes and environments; however, the presence or absence of antiherbivore defenses is a major factor determining insect resistance (Chen et al., 2009; Smith et al., 2012).

Maize has also been a model for identification of molecules from insects that trigger protective responses. Maize bioassays for elicited VOC production using activity-guided fractionation efforts enabled discoveries of the first defined biomolecules from insect oral secretions (OSs) that act as defense elicitors, termed herbivore-associated molecular patterns (HAMPs) (Alborn et al., 1997; Felton and Tumlinson, 2008). Originally isolated from *S. exigua*, fatty acid–amino acid (aa) conjugates (FACs) are a family of molecules based on the conjugation of plant-derived linolenic acid to either glutamine or glutamate in the insect gut (Alborn et al., 1997; Halitschke et al., 2001; Lait et al., 2003; Pare et al., 1998; Yoshinaga et al., 2008). Among the naturally occurring FACs, 17-hydroxy *N*-linolenoyl L-glutamine (volicitin) and *N*-linolenoyl L-glutamine (Gln-18:3) are commonly the most highly abundant and potent elicitors of foliar volatile emissions (Mori and Yoshinaga, 2011; Schmelz et al., 2009; Turlings et al., 2000; Yoshinaga et al., 2008, 2010). FACs occur in diverse insects and play a nutritional role by increasing nitrogen assimilation efficiency in midgut tissues (Mori and Yoshinaga, 2011; Yoshinaga et al., 2007, 2008). FACs are potent defense elicitors in diverse plants, including maize, rice (*Oryza sativa*), soybean (*Glycine max*), *Medicago*, and many solanaceous species (Gomez et al., 2005; Grissett et al., 2020; Schmelz et al., 2009; Shinya et al., 2016; Turlings et al., 2000; Wu and Baldwin, 2009). Although FACs have been the dominant HAMP studied in maize, additional insect-associated molecules also promote maize defenses. Disulfooxy fatty acids, termed caeliferins, present in the American bird grasshopper (*Schistocerca americana*) and microbes associated with the insect digestive tract elicit antiherbivore defense responses in maize, while chitinases in *Helicoverpa zea* frass suppress antiherbivore defense responses (Alborn et al., 2007; Ray et al., 2015, 2016; Wang et al., 2018a, 2018b). Finally, plant hormones contained in both larval OSs and frass modulate maize immunity as well (Acevedo et al., 2019; Dafoe et al., 2013). While these diverse insect-associated molecules contribute to elicitation of maize defenses, maize is insensitive to numerous other oral cues from chewing insects such as Lepidopteran-produced inceptin, *Helicoverpa*-associated glucose oxidase and ATPases, and β-glucosidase from *Pieris brassicae* (Mattiacci et al., 1995; Schmelz et al., 2007; Tian et al., 2012; Wang et al., 2018a, b).

Maize signaling promoted by HAMPs is mediated and amplified by an array of endogenous signals (Huffaker et al., 2013; Poretsky et al., 2020; Schmelz, 2015; Schmelz et al., 2003). Generally, mechanical wounding of plant

tissue leads to the release of damage-associated molecular patterns (DAMPs), including oligogalacturonic acid, extracellular ATP, and peptides similar to systemin and plant elicitor peptides (Peps) (Huffaker et al., 2006; Orozco-Cardenas and Ryan, 1999; Pearce et al., 1991; Tanaka et al., 2014). In addition to HAMPs, DAMPs further amplify wounding-mediated production of phytohormones, including jasmonates (JAs) and ethylene (ET), to regulate herbivore-associated defense responses (Diezel et al., 2009; Erb et al., 2012; Schmelz et al., 2003; Shinya et al., 2018). Additionally, rapid signaling cascades involving glutamate-like receptor (GLR) proteins, MAP kinase (MAPK) cascades, Ca^{2+} influxes, and bursts of reactive oxygen species (ROS) collectively contribute to the propagation of immune signaling both spatially and temporally (Erb and Reymond, 2019). As amplifiers of maize immune signaling, maize encodes 13 ZmPeps contained in six precursor protein genes (Huffaker et al., 2011, 2013; Poretsky et al., 2020). Peps in rice (OsPeps) have also been demonstrated to protect against herbivores and act synergistically with HAMPs to generate stronger responses (Shinya et al., 2018). While the potency of ZmPep family members varies in the magnitude of elicited responses, the promotion of JA and ET production, VOC emission, and accumulation of transcripts encoding proteinase inhibitors and other defense proteins is shared (Poretsky et al., 2020). Within the ZmPep family, ZmPep3 is the most potent DAMP signal (Huffaker et al., 2013; Poretsky et al., 2020). ZmPeps are recognized by two leucine-rich repeat (LRR) receptor-like kinases (RLKs), ZmPEPR1 and ZmPEPR2, and plants with *Zmpepr* mutations produce fewer volatiles and are less capable of generating a protective response against *Spodoptera* larvae after ZmPep treatment (Poretsky et al., 2020). This is consistent with other studies demonstrating that impairments to wound and DAMP signaling commonly result in reduced herbivore resistance, supporting functional roles for interconnected signaling pathways (Onkokesung et al., 2010; Orozco-Cardenas et al., 1993; Poretsky et al., 2020; Thaler et al., 2002; Wang et al., 2018a,b).

Direct comparisons in maize of exogenous HAMPs and endogenous DAMPs, such as Gln-18:3 and ZmPep3, revealed striking overlap in the elicitation of defense and protective responses against *Spodoptera* herbivores (Huffaker et al., 2013). Given the highly similar activation of defenses, our current research effort seeks to better understand early maize responses to ZmPep3 and Gln-18:3 and comprehensively assess transcriptome-wide overlap and response divergence. Using transcriptional profiling we demonstrated that while ZmPep3 is a more potent signal, both ZmPep3 and Gln-18:3 promote highly similar reprogramming responses at 2 h, largely represented by transcripts encoding signaling proteins. Towards the goal of uncoupling highly similar HAMP and DAMP responses, characterization of ZmPep3 and Gln-18:3 sensitivity across diverse maize lines revealed defined maize inbred lines specifically insensitive to Gln-18:3. In a parallel, unbiased, and focused approach to candidate gene discovery, we then used forward genetics to better understand FAC response sensitivity. Association mapping using the intermated B73 × Mo17 (IBM) recombinant inbred line (RIL) population enabled the identification of a single locus specifically associated with response sensitivity to Gln-18:3, but not ZmPep3. Fine-mapping and characterization of this locus led to identification of an LRR-RLK gene, termed *FAC SENSITIVITY ASSOCIATED* (*ZmFACS*), as the top candidate consistent with contributions to Gln-18:3 response sensitivity. Using two diverse approaches, our work expands the current knowledge of maize genes involved in early signaling responses to defined HAMPs and DAMPs. Furthermore, we provide a long-sought path to uncoupling linked HAMP and DAMP responses in plants.

RESULTS

Comparison of early HAMP- and DAMP-elicited transcriptional changes in maize

Comparative analyses of canonical defense responses against herbivores in maize and rice have revealed considerable connections between HAMP- and DAMP-elicited responses, consistent with shared signaling pathways (Huffaker et al., 2013; Shinya et al., 2018). To confirm that Gln-18:3 and ZmPep3 elicit antiherbivore defenses in the maize B73 inbred similar to previous observations in hybrid sweet corn (Huffaker et al., 2013), B73 seedlings were treated with water, ZmPep3, and Gln-18:3, and VOC emission was measured 16 h later. In support of earlier findings, both ZmPep3 and Gln-18:3 treatments result in significantly higher levels of VOC emission compared to water-treated samples (Figure 1a). At equal concentrations ZmPep3 induces higher volatile production than Gln-18:3 (Figure 1a). To comprehensively compare early responses to Peps and FACs, B73 leaves were treated with water, ZmPep3, and Gln-18:3 and RNA sequencing (RNA-seq)-based transcriptomes were generated for the 2-h time point (Table S1). Analyses of the number of differentially expressed genes (DEGs) as compared to water-treated controls showed a similar pattern to that observed for elicitor-induced VOC emission, namely a greater number of ZmPep3-elicited DEGs (1703) compared to Gln-18:3-elicited DEGs (358) (Figure 1b, Table S2). While a quantitative difference in ZmPep3 and Gln-18:3 DEGs exists, Euler diagram analyses of the overlap between the combined up- and downregulated DEGs revealed that Gln-18:3 responses display a high degree of overlap with ZmPep3 responses (Figure 1c, Table S2). Specifically, 87% of all Gln-18:3 DEGs were also differentially expressed following ZmPep3 treatment. In the context of upregulated DEGs,

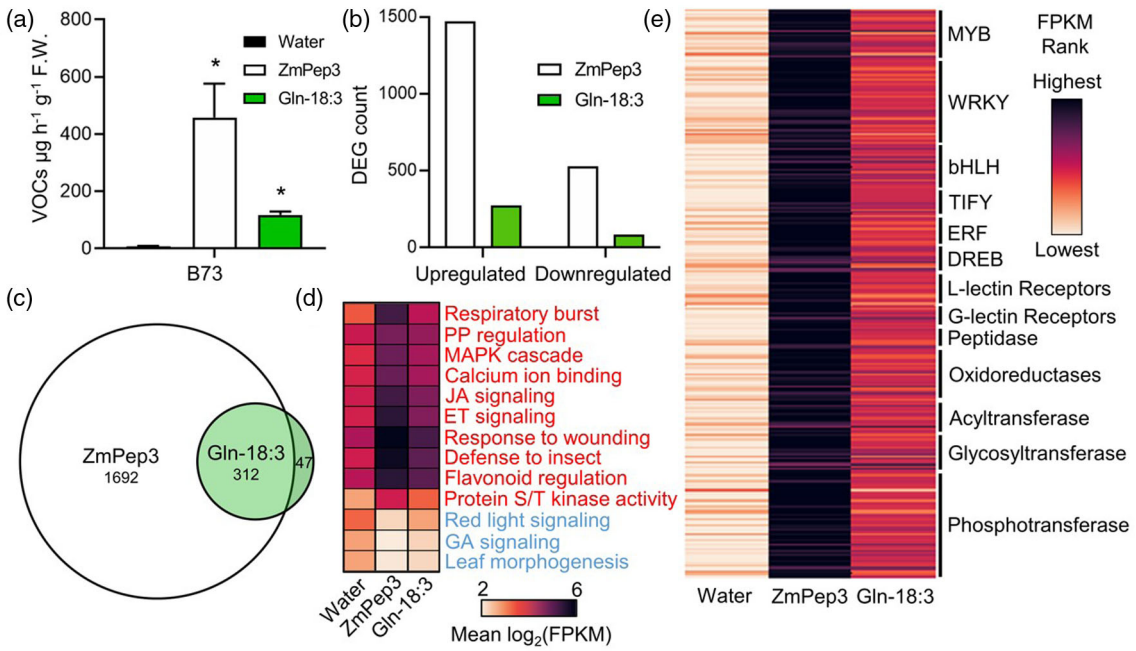

Figure 1. Comparative analysis of ZmPep3- and Gln-18:3-induced VOC emission and early transcriptional changes. (a) Analysis of total elicitor-induced VOC emission 16 h after treatment of B73 leaves with water, 5 µM ZmPep3, or 5 µM Gln-18:3. Total VOC is represented by the sum of (*Z*)-3-hexenyl acetate, linalool, (3*E*)-4,8-dimethyl-1,3,7-nonatriene (DMNT), β-caryophyllene, (*E*)-α-bergamotene, (*E*)-β-farnesene, and *E*-nerolidol. (b) Measurement of the number of differentially expressed genes (DEGs) following elicitor-induced 2-h treatments measured by RNA-seq. (c) Euler diagram representing the overlap of the combined upregulated and downregulated DEGs. (d) Summary heatmap of the mean $\log_2$(FPKM) data of all ZmPep3- and Gln-18:3-induced DEGs in selected enriched GO terms. Enriched GO terms for upregulated DEGs are in a red font and downregulated DEGs are in a blue font. PP, phenylpropanoid. (e) Summary heatmap of all ZmPep3-upregulated DEGs assigned to their enriched MAPMAN bins with more than 10 DEGs in respective bins. Row colors are based on the treatment mean of the ranked FPKM values for each gene. For all treatments shown $n = 4$ and error bars represent SEMs. Student *t*-tests (two-tailed distribution, unpaired) were used for the detection of significant differences. Asterisks indicate significant differences with $P < 0.05$; ns, not significant.

Gln-18:3-elicited transcripts displayed 92.4% overlap with ZmPep3 responses (Figure S1). Further supporting largely shared processes, none of the upregulated DEGs in either treatment were downregulated in the other treatment, and *vice versa* (Figure S1).

To consider biological processes differentially regulated following ZmPep3 and Gln-18:3 treatment, both the maize Phytozome Gene Ontology (GO) and maize MAPMAN annotations were used (Goodstein et al., 2012; The Gene Ontology Consortium, 2019; Thimm et al., 2004). To visualize large-scale differences in the mean expression values of numerous enriched GO terms, a heatmap representing the mean expression values of the DEGs associated with each term was generated (Figure 1d, Table S3). Among the GO terms enriched in the upregulated DEGs were terms associated with defense signaling and defense responses, including phytohormone and kinase signaling, specialized metabolism, response to wounding, and defense to insects, that had the highest mean expression in the ZmPep3-treated leaves followed by the Gln-18:3-treated leaves (Figure 1d, Table S3). Among the GO terms enriched in the downregulated DEGs were terms associated with growth and development, including red light signaling, gibberellic acid (GA) signaling, and regulation of leaf morphogenesis, that had the lowest mean expression in the ZmPep3-treated leaves followed by Gln-18:3 treatment (Figure 1d, Table S3). In contrast to GO terms, the maize MAPMAN bin annotation provides more specific pathway gene groups (Thimm et al., 2004). Enrichment analysis revealed a diverse set of MAPMAN bins associated with ZmPep3- and Gln-18:3-upregulated genes, including genes involved in pathogen-associated molecular pattern (PAMP)-triggered immunity or indole biosynthesis and genes encoding MAPKs, guard cell S-type anion channels (SLACs), PAMP-induced secreted peptide (PIP) and PIP-LIKE (PIPL) signaling L-lectin receptors, and transcription factors (TFs) in the myeloblastosis (MYB), WRKY, basic helix–loop–helix (bHLH), dehydration-responsive element binding (DREB), and TIFY families (Table S4). Enriched MAPMAN bins associated with ZmPep3- and Gln-18:3-downregulated genes included PHYTOCHROME B, cell cycle and abscisic acid (ABA) signaling, biosynthesis of gibberellic acid (GA) and brassinosteroids (BR), and TFs from the MYB, C2H2, bHLH, and Trihelix families (Table S4). Of the 51 enriched bins for ZmPep3-upregulated genes, only 13 contained more than 10 DEGs, which were associated with six different TF families, L- and G-lectin receptor families, and enzymes with peptidase, oxidoreductase, acyltransferase, glycosyltransferase, and phosphotransferase activity (Figure 1e, Table S4). Additionally, heatmap visualization of

the ranked fragments per kilobase of transcript per million mapped reads (FPKM) expression data of all ZmPep3-upregulated genes in these enriched bins showed that the majority of ZmPep3-upregulated DEGs also exhibited higher mean expression following Gln-18:3 treatment compared to water treatment (Figure 1e). Similarly, a global comparison of all DEGs using the ranked FPKM expression data showed that over 95% of ZmPep3 DEGs displayed an intermediate Gln-18:3 ranked mean expression, between ZmPep3 and water, despite a nearly 5-fold greater number of ZmPep3 DEGs compared to Gln-18:3 (Table S5). Overall trends in early transcriptional responses following ZmPep3 and Gln-18:3 treatment support highly similar regulation.

Identification of differentially expressed genes after 2 h of HAMP and DAMP treatment

A comparative analysis of the ZmPep3 and Gln-18:3 DEGs was used to probe transcriptional changes in gene groups and pathways with putative roles in regulation of antiherbivore defenses. MAPMAN pathway annotation and gene descriptions were used to group genes with shared functions (Thimm et al., 2004). Groups included genes involved in signal transduction across membranes, MAPK signaling, phytohormone biosynthesis and signaling, TFs, cytoplasmic signaling, and antiherbivore defenses (Figure 2, Table S6). After identifying the ZmPep3 DEGs in selected groups, a heatmap was generated illustrating the fold change values of the DEGs, including the number of DEGs compared to the total number of genes in each group (Figure 2, Table S6). Genes that were also significantly differentially regulated following Gln-18:3 treatment were marked using thatched, cyan-colored boxes (Figure 2, Table S6). Together this assembled landscape of signaling-related genes includes LRR-RLKs and LRR-receptor-like proteins (LRR-RLPs), lectin receptors, GLRs, respiratory burst oxidase homologs (RBOHs), calcium-dependent protein kinases (CDPKs), receptor-like cytoplasmic kinases

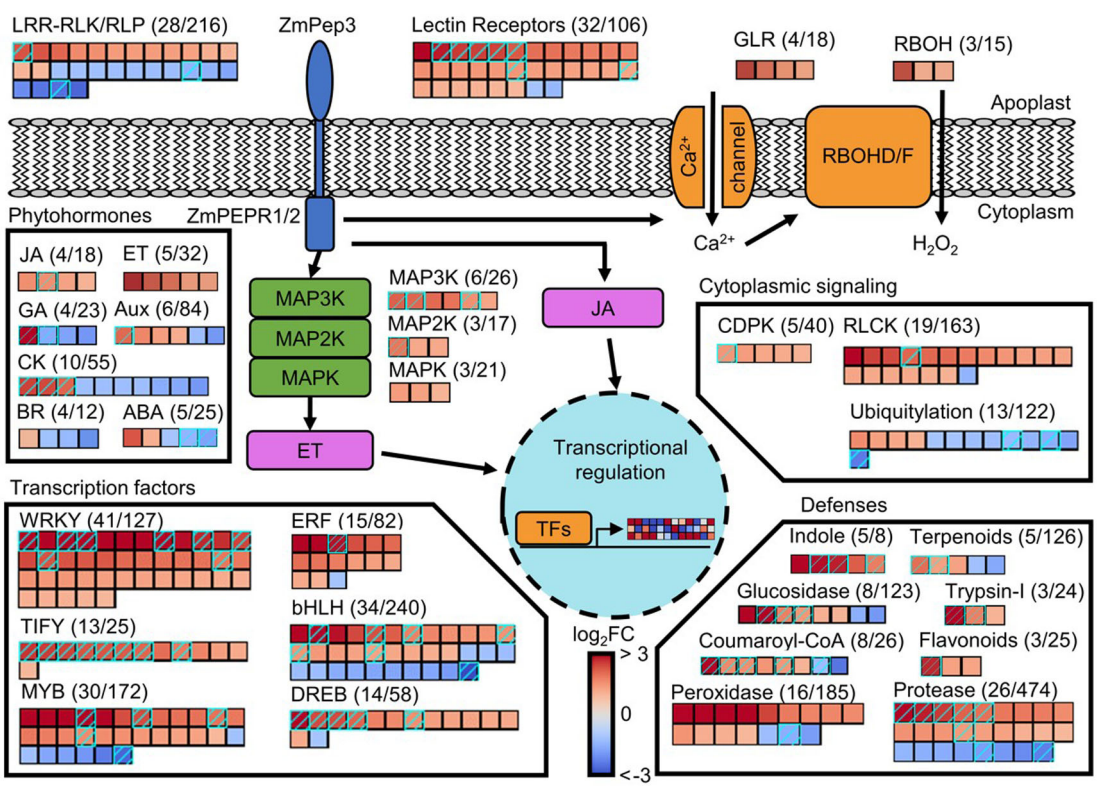

Figure 2. Early elicitor-induced transcriptional regulation of multiple components associated with antiherbivore responses. Heatmaps of gene groups represent $\log_2$(fold change) data from RNA-seq results of ZmPep3-induced differentially expressed genes and are based on the *Zea mays* RefGen_V4 MAPMAN annotation. Hatched cyan boxes indicate genes that were also significantly differentially expressed following Gln-18:3 treatment. The selected gene groups were obtained either from the MAPMAN bin annotations or from searching selected keywords in the MAPMAN gene descriptions in the case of the glucosidase, peroxidase, protease, and trypsin inhibitor (Trypsin-I) gene groups. Parentheses next to each abbreviated group title are the numbers of ZmPep3-elicited DEGs compared to the size of the gene group. LRR-RLK/RLP, leucine-rich repeat receptor-like kinase/receptor-like protein; GLR, glutamate-like receptor; RBOG, respiratory burst oxidase homolog; JA, jasmonic acid; ET, ethylene; GA, gibberellic acid; Aux, auxin; CK, cytokinins; BR, brassinosteroids; ABA, abscisic acid; MAPKs, mitogen-activated protein kinase; CDPK, calcium-dependent protein kinase; RLCK, receptor-like cytoplasmic kinase; TF, transcription factor; ERF, ethylene response factor; Trypsin-I, trypsin inhibitor. All associated B73 RefGen_V4 gene IDs and transcript $\log_2$(fold change) data underlying this figure are detailed in Table S6.

(RLCKs), genes involved in ubiquitylation, MAPK-associated genes, and phytohormone biosynthetic genes involved in JA, ET, and other pathways. Among the genes involved in signaling, the lectin receptors had the highest proportion of DEGs compared to the group size (30%), while the LRR-RLK/RLP and ubiquitylation groups had among the highest proportion of DEGs split between the number of upregulated and downregulated DEGs (50 and 30% were upregulated, respectively). For bins involved in phytohormone biosynthesis and signaling, genes associated with JA and ET bins were upregulated, whereas the majority of those in GA, auxin, cytokinin (CK), and ABA groups were downregulated. A large proportion of WRKY and TIFY TF groups were upregulated compared to the size of the group (32 and 52%, respectively), while the DEGs in the bHLH and MYB TF groups were split between upregulated and downregulated genes (61 and 76% were upregulated, respectively). Groups of genes with either established or putative roles in antiherbivore defenses include genes involved in indole, terpenoid, flavonoid, and coumaroyl-CoA biosynthetic pathways, as well as trypsin inhibitors, glucosidases, peroxidases, and proteases. Among defense-related genes, groups associated with indole and coumaroyl-CoA biosynthetic pathways had among the highest proportion of ZmPep3 DEGs compared to the size of the group (62 and 30%, respectively). The TIFY TF group and the coumaroyl-CoA biosynthetic pathway group displayed high proportions of genes that were also upregulated by Gln-18:3 in comparison to ZmPep3 DEGs (61 and 62%, respectively) (Figure 2).

Assessment of genetic variation in sensitivity to ZmPep3 and Gln-18:3

Large-scale overlap in early transcriptional regulation following ZmPep3 and Gln-18:3 treatments supports the hypothesis that defined HAMPs and DAMPs activate maize antiherbivore defenses through highly similar signaling pathways. Previous work on herbivore-induced VOCs revealed significant variation among genetically diverse maize lines (Degen et al., 2004). To narrow the number of candidate genes that have the potential to uncouple ZmPep3 and Gln-18:3 responses, maize inbred lines with reference genomes were analyzed for differential responses to the two elicitors. We hypothesized that the observed response phenotype variation associated with herbivore-induced VOCs could be due to genetic impairments in HAMP responsiveness, DAMP responsiveness, or shared downstream signaling components. To identify genetic variability in either Pep- or FAC-elicited responses, 27 maize inbred lines were screened for ZmPep3- and Gln-18:3-elicited volatile sesquiterpene production. This set included B73, Mo17, and W22 inbred lines and parent lines of the nested association mapping (NAM) population, which collectively represent over 90% of maize genetic diversity (McMullen et al., 2009). CML52 could not be included due to insufficient seed germination. Observed B73 responses were typical of most examined inbred lines and emitted significantly more sesquiterpene volatiles after both ZmPep3 and Gln-18:3 treatments compared to water treatment alone (Figure 3a). Nineteen of the 27 lines responded similarly with increased sesquiterpene emissions to both treatments (Figure 3a). Four inbred lines, namely HP301, CML333, MS71, and Ky21, failed to emit statistically significant increases in sesquiterpene volatiles in response to either ZmPep3 or Gln-18:3, suggesting the existence of potential mutations in shared signaling pathways (Figure 3b). Importantly, four inbred lines, namely CML103, NC350, CML69, and Mo17, emitted significant levels of sesquiterpene volatiles after ZmPep3 treatment but produced no response after Gln-18:3 treatment (Figure 3c). The final response phenotype (Figure 3c) is consistent with selective FAC insensitivity and the existence of a genetic basis that underlies signaling nodes able to uncouple FAC- and Pep-elicited responses.

Differential responses in B73 and Mo17 enable forward genetics and the establishment of an FAC sensitivity-associated locus

As an inbred line specifically insensitive to Gln-18:3, Mo17 was selected for further study due to the availability of established genetic resources with RILs, near isogenic lines (NILs), and high-density genotypic markers (Eichten et al., 2011; Lee et al., 2002; Romay et al., 2013). To confirm that Mo17 is specifically Gln-18:3-insensitive, total VOCs were measured after treatment with water, ZmPep3, and Gln-18:3. As observed in the prior experiment, VOC emission was significantly increased after treatment with ZmPep3 in both B73 and Mo17, but only B73 emitted significantly more VOCs after Gln-18:3 treatment (Figure 4a). Because elicitor-induced VOC emission is a relatively late response measured 16 h after treatment, analyzed differences in Mo17 responses occur long after application of the signals. To assess whether Mo17 displays insensitivity to Gln-18:3 during earlier signaling events, both B73 and Mo17 were treated for 2 h with water, ZmPep3, and Gln-18:3 and analyzed for ET emission. Consistent with VOC emission, B73 emitted significantly more ET following both ZmPep3 and Gln-18:3 treatments, while Mo17 emitted significantly more ET following ZmPep3 but not following Gln-18:3 treatment (Figure 4b). Using both early and late markers for signal activation, our results support the hypothesis that Pep responsiveness in Mo17 is decoupled from FAC responsiveness and that genetic variation in FAC-specific signaling components exists.

Based on differential FAC sensitivity between B73 and Mo17, the IBM RIL population (Lee et al., 2002) was used for genetic mapping of FAC sensitivity. Using 222 IBM RILs, ZmPep3- and Gln-18:3-induced leaf VOCs were

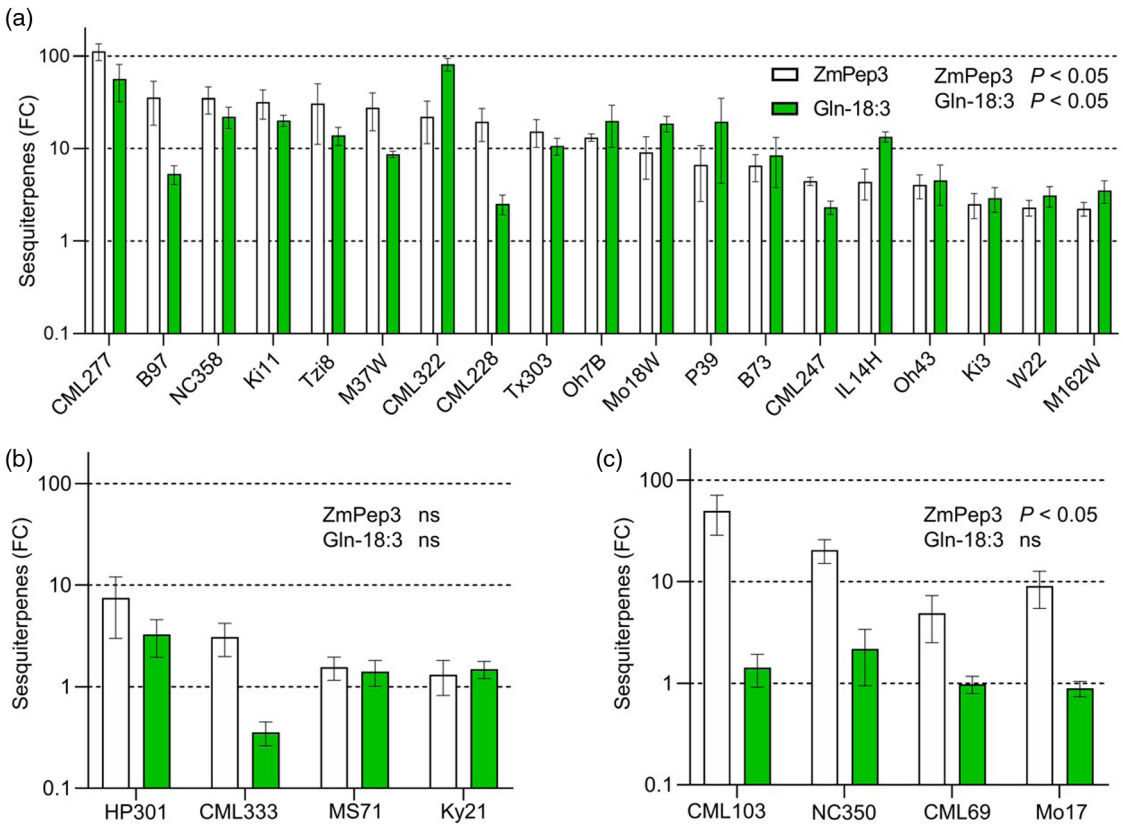

Figure 3. Diverse maize inbred lines display significant variation in HAMP- and DAMP-elicited defense responses of volatile sesquiterpenes. A total of 27 maize inbred lines including B73, Mo17, W22, and the nested association mapping parent lines were analyzed for elicitor-induced volatile sesquiterpene emission. Maize leaves were treated for 16 h with water, 1 μM ZmPep3, or 1 μM Gln-18:3 and volatiles were analyzed by gas chromatography. Results are presented as the fold change (FC) in elicitor-induced sesquiterpene emission compared to the water treatment. Sesquiterpenes are defined as the sum of β-caryophyllene, (*E*)-α-bergamotene, (*E*)-β-farnesene, and *E*-nerolidol. For all treatments shown $n = 4$ biological replicates and error bars represent SEMs. Significance of elicitor-induced sesquiterpene emission was determined by Student *t*-tests (two-tailed distribution, unpaired) for each line, and was used to classify the maize inbred lines into three categories: (a) lines with both significant HAMP and DAMP elicitor-induced responses ($P < 0.05$), (b) lines where both elicitor-induced responses were not statistically significant (ns), and (c) lines with significant ZmPep3-induced responses but not significant Gln-18:3-induced responses.

analyzed and compared to water-treated control plants. Association mapping was conducted based on the fold change values of ZmPep3- and Gln-18:3-induced VOC emission as compared to water-treated leaves (Table S7). The single-nucleotide polymorphism (SNP)-based genetic marker map (B73 RefGen_V2) of the IBM RILs (www.panzea.org, July 2012 Imputed All Zea GBS final build) was used for association mapping (Ding et al., 2020). The general linear model (GLM) procedure in TASSEL 5.0 was used to calculate the statistical significance of SNP associations using the fold change values of ZmPep3- and Gln-18:3-induced VOCs as traits (Bradbury et al., 2007; Romay et al., 2013). Association mapping revealed a single locus on chromosome 4 as significantly associated with total VOC emission specifically elicited by Gln-18:3 and not by ZmPep3 (Figure 4c). The FAC sensitivity locus coordinates are based on adjusted *P*-values ($P < 0.05$; Bonferroni correction for multiple comparisons), and the locus was defined as the region between B73 RefGen_V2 SNPs S4_237390439 and S4_238691014 (1.9 Mbp), which corresponds to the B73 RefGen_V4 region between the genes *Zm00001d053820* and *Zm00001d053932*, containing 81 genes (Figure 4c, Table S8). Box-plot visualization of the ZmPep3 and Gln-18:3 VOC fold change data split according to allele identity at the most highly associated SNP (S4_237322925) and confirmed that the FAC sensitivity locus was obtained due to Gln-18:3 sensitivity in the presence of the B73 allele and Gln-18:3 insensitivity in the presence of the Mo17 allele (Figure 4d). To ensure that the Gln-18:3-specific association mapping result (Figure 4c) was not driven by variation in a single VOC biosynthetic pathway, we investigated (*Z*)-3-hexenyl acetate, (*E*)-4,8-dimethyl-1,3,7-nonatriene (DMNT), and *E*-β-farnesene as separate mapping traits and obtained identical results consistent with a Mo17 lesion impacting early signal propagation (Figure S2a–f).

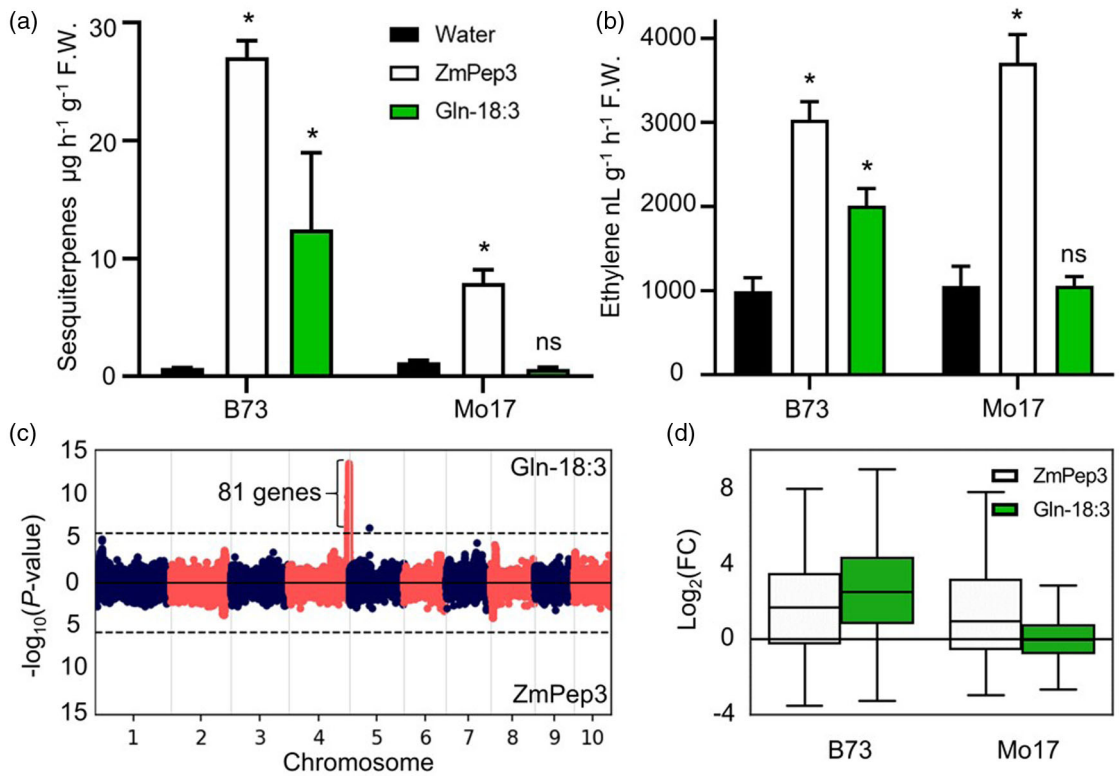

Figure 4. Forward genetics approaches using association analyses were used to identify a maize FAC sensitivity locus based on Gln-18:3-specific response impairments in Mo17. (a) Average (n = 4, +SEM) total sesquiterpene emission after 16 h and (b) average ethylene (n = 6, +SEM) emission after 2 h following treatment of B73 and Mo17 leaf 5 with water, 5 µM ZmPep3, or 5 µM Gln-18:3. Sesquiterpenes are specifically the sum of β-caryophyllene, (*E*)-α-bergamotene, (*E*)-β-farnesene, and *E*-nerolidol. (c) Metabolite-based association analyses using 222 intermated B73 × Mo17 (IBM) recombinant inbred lines (RILs) and elicited VOC fold change values as traits derived from leaf 5 treated with water, 1 µM ZmPep3, or 1 µM Gln-18:3. VOCs were analyzed 16 h after treatments. Imputed IBM RIL SNP markers (165 033) were obtained from the Panzea project (www.panzea.org). Fold change values were calculated using the sum of the total VOC, defined as the combination of (*Z*)-3-hexenyl acetate, linalool, (3*E*)-4,8-dimethyl-1,3,7-nonatriene (DMNT), β-caryophyllene, (*E*)-α-bergamotene, (*E*)-β-farnesene, and *E*-nerolidol. (d) Box-plots showing the distribution of elicitor-induced fold change VOC emission at the top SNP (B73 RefGen_V2, S4_237322925) associated with FAC sensitivity across IBM RILs. Dashed lines in the Manhattan plots indicate a significance cutoff of $P < 0.05$ based on Bonferroni correction. Numbers of genes are based on B73 RefGen_V4 annotations. Error bars represent SEMs. Student *t*-tests (two-tailed distribution, unpaired) were used for the detection of significant differences. Asterisks indicate significant differences with $P < 0.05$. ns, not significant.

NILs narrow the maize chromosome 4 locus associated with FAC sensitivity

A second independent genetic population derived from B73 and Mo17 was used to provide additional support for the FAC sensitivity locus. The B73 x Mo17 NILs contain small introgression regions from one of the parent genomes into the other nearly uniform genetic background (Eichten et al., 2011). Two NILs, b050 and b154, were identified as containing an introgression of the Mo17 genome into the B73 background within the FAC sensitivity locus and were screened for ZmPep3- and Gln-18:3-elicited VOC production. Both NILs emitted significantly more VOCs after treatment with ZmPep3, but only b154 emitted significantly more VOCs after treatment with Gln-18:3 (Figure 5a). These results further support the IBM RIL-derived FAC sensitivity locus (Figure 4c) and importantly narrow the consideration of candidate genes by reducing the locus to 1.5 Mbps containing 54 genes based on the B73 RefGen_V4 annotation between 242.2 Mbp and 243.7 Mpb (Figure 5b, Table S8).

Fine-mapping the FAC sensitivity locus using a newly generated IBM RIL marker map

IBM RILs provide high-resolution resources to investigate the genetic basis of traits associated with development and disease, in part due to five generations of intermating before selfing to create a high-resolution RIL mapping population (Lee et al., 2002; Liu et al., 2020). Given considerable investments in the IBM RIL population, improved resolution genetic marker maps are possible using genotype-by-sequencing (GBS) approaches to identify additional sites of recombination and associated SNPs from DNA sequence data (Romay et al., 2013). To expand this direction, we obtained and analyzed the raw RNA-seq data (PRJNA179160) of a subset of 105 of the 302 IBM RILs from an existing study on the regulation of gene

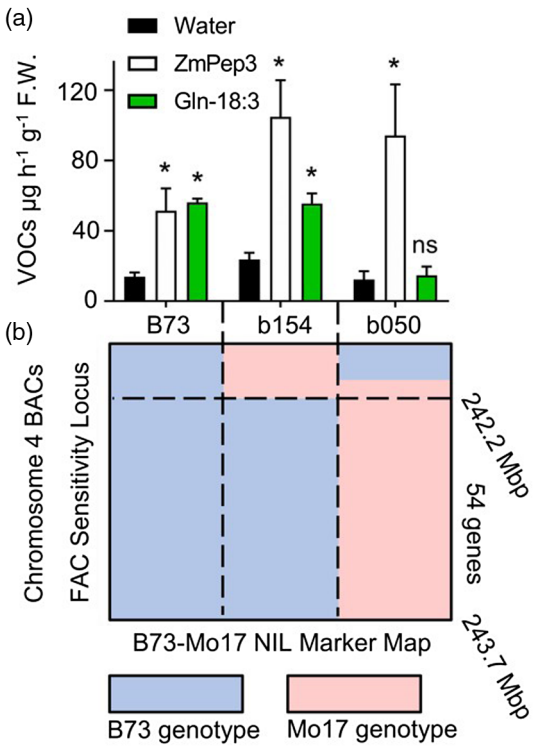

Figure 5. The maize FAC sensitivity locus was narrowed using IBM near isogenic lines (NILs). (a) Average (n = 4, +SEM) total elicitor-induced VOC emission 16 h after treatment of B73, b154, and b050 leaves with water, 5 μM ZmPep3, or 5 μM Gln-18:3. Total VOC is represented by the sum of (*Z*)-3-hexenyl acetate, linalool, (3*E*)-4,8-dimethyl-1,3,7-nonatriene (DMNT), β-caryophyllene, (*E*)-α-bergamotene, (*E*)-β-farnesene, and *E*-nerolidol. (b) Genetic map of the specific B73-Mo17 NILs illustrates two lines, b154 and b050, containing an introgression of the Mo17 genotype into the B73 genetic background within the FAC sensitivity locus. Coordinates and gene number are based on the B73 RefGen_V4 annotation. Student *t*-tests (two-tailed distribution, unpaired) were used for the detection of significant differences. Asterisks indicate significant differences with $P < 0.05$. ns, not significant.

expression in 2-week-old seedlings (Li et al., 2013). Raw data were aligned to the B73 RefGen_V4 genome and used for variant calling. The resulting SNPs were filtered followed by aggregation of all SNPs to a B73 and Mo17 gene-based marker map containing a total of 10 043 marker genes (Figure 6a, Table S9). Association analyses were performed using the Gln-18:3-induced VOC fold change data, similar to the previous approach (Figure 4c), using a subset of 86 IBM RIL lines (Table S7) for which the refined marker data were generated. After using the Bonferroni correction for multiple testing and selecting marker genes with a significant threshold of $P < 0.05$, the FAC sensitivity locus was fine-mapped to a greatly narrowed locus between 242.2 Mbp and 242.8 Mbp (B73 RefGen_V4) containing only 19 genes (Figure 6b, Table S8). To assess the accuracy of the gene marker map at the FAC sensitivity locus, the allele counts of all SNPs in the region were aggregated and grouped based on the called genotype. These results indicated that higher allele counts matched the predicted SNP genotype, while counts of the alternative alleles were generally close to zero (Figure 6c). The SNPs that were called as heterozygous were similarly distributed in both the B73 and Mo17 allele counts (Figure 6c). To verify the fine-mapping results, three IBM RILs for which a recombination event was detected within the fine-mapped region (B73 RefGen_V4: 242.2 Mbp and 242.8 Mbp) were tested for elicited VOC emission following treatment with water, ZmPep3, and Gln-18:3. In agreement with our refined IBM RIL-based fine-mapping results, while all lines had significant ZmPep3-induced VOCs, significant Gln-18:3-induced VOCs were only observed when the genotype at the fine-mapped region was B73 (Figure 6d,e). Among the 19 predicted genes within the narrowed FAC sensitivity locus (Table S8), multiple genes exist that theoretically have the potential to impact signaling and transcriptionally mediated responses. These include genes predicted to encode proteins with DNA- or RNA-binding activity (*Zm00001d053855*, *Zm00001d053860*), ATP- or GTP-binding activity (*Zm00001d053857*, *Zm00001d053858*, *Zm00001d053861*), or RNA polymerase-related activity (*Zm00001d053872*, *Zm00001d053874*) and protein kinase superfamily proteins (*Zm00001d053853*, *Zm00001d053876*). Curiously, at the center of the 19-gene locus exist two genes annotated as LRR-RLKs, namely *Zm00001d053866* and *Zm00001d053867*. The predicted *Zm00001d053866* sequence displays considerable physical overlap with the intact LRR-RLK-encoding gene *Zm00001d053867* and thus is consistent with a gene prediction algorithm error resulting in misannotation of *Zm00001d053866*. Given the physical genetic position and common role in early signal transduction events mediated by LRR-RLK family members (Reymond, 2021), we selected the intact *Zm00001d053867* gene, termed *FAC SENSITIVITY ASSOCIATED* (*ZmFACS*), as the top candidate for further assessment in mediating FAC sensitivity (Figure 6f, Table S8).

ZmFACS belongs to the same gene family as the rice receptor *OsLRR-RLK1*, which positively regulates antiherbivore responses

Of the gene candidates present in the FAC sensitivity locus, *ZmFACS* exists as a member of a receptor gene family that includes the rice gene *OsLRR-RLK1*, which was a candidate selected from a transcriptional profiling study and characterized as a positive regulator of rice antiherbivore responses to diverse lepidoptera attacks and crude FAW OSs (Figure 7a) (Hu et al., 2018; Zhou et al., 2011). ZmFACS and OsLRR-RLK1 belong to the LRR-Xb subfamily of LRR-RLKs, which also includes the phytosulfokine (PSKR1/2) and PSY1 receptors (PSY1R), with PSY1R being the more closely related Arabidopsis LRR-RLK to ZmFACS and OsLRR-RLK1 (Figure 7a) (Hu et al., 2018; Shiu et al., 2004). *OsLRR-RLK1*

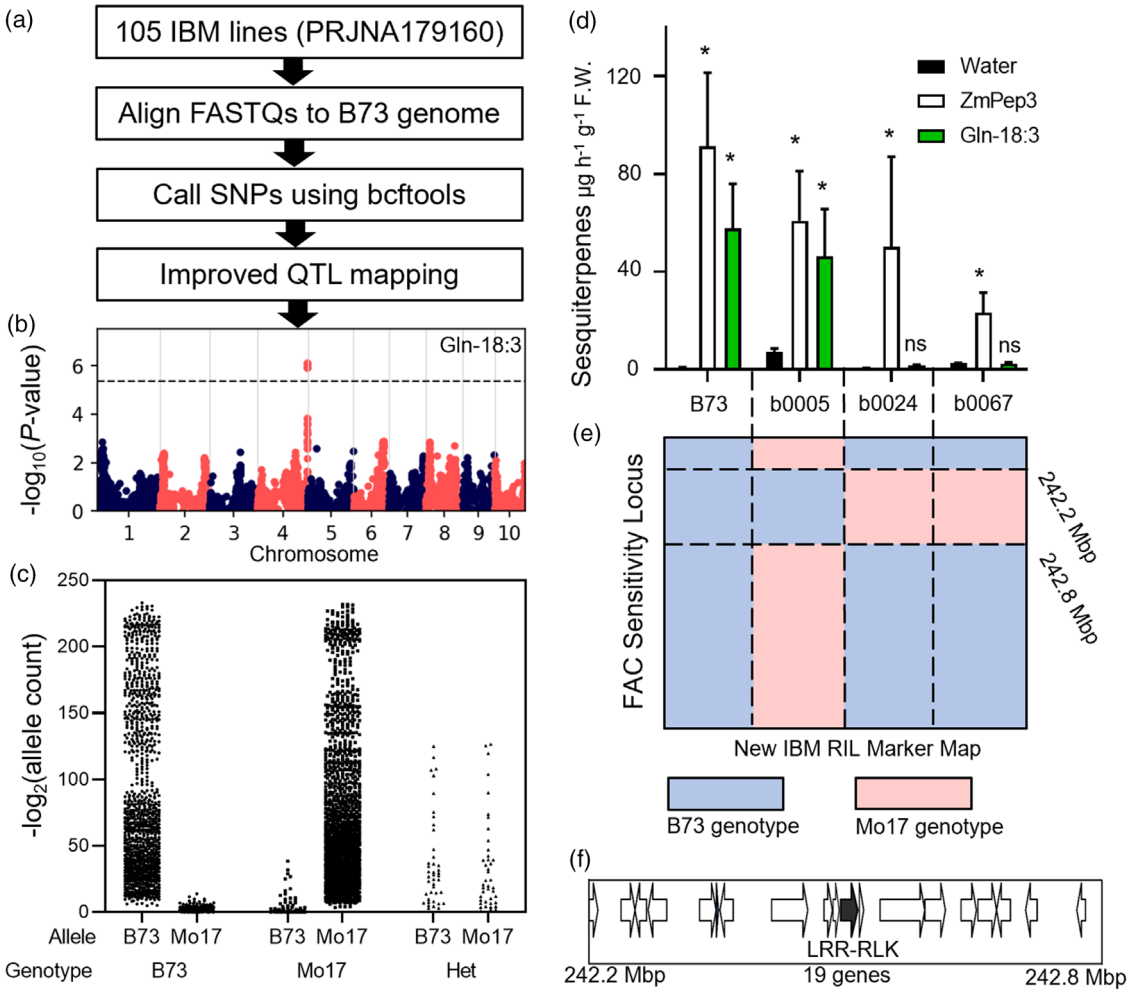

Figure 6. Fine-mapping the FAC sensitivity locus using a newly generated marker map for 105 IBM RILs. (a) Summarized procedural workflow describing the creation of the new IBM RIL marker map using RNA-seq data from 105 IBM RILs obtained from NCBI aligned to the B73 RefGen_4 genome. (b) Association analyses using the new IBM RIL map (B73 Ref Gen_V4; 10,043 marker genes) with total VOC fold change values from leaf 5 of 86 RILs treated with water, 1 µM ZmPep3, or 1 µM Gln-18:3 analyzed 16 h after treatment. The association analysis (general linear model) with newly assigned markers and VOC fold change traits follows from Figure 4c. Dashed lines in Manhattan plots indicate a significance cutoff of $P < 0.05$ based on Bonferroni correction. The most highly associated gene marker is Zm00001d053868. (c) Aggregated allele counts of all SNPs within the FAC sensitivity locus that were used for generating the new IBM RIL marker map compared to the final assigned marker genotype. Het, heterozygous. (d) Average ($n = 3$, +SEM) elicitor-induced sesquiterpene emission, as measured by the sum of β-caryophyllene, (*E*)-α-bergamotene, and (*E*)-β-farnesene 16 h after treatment of B73 and IBM RIL b0005, b0024, and b0067 leaves with water, 5 µM ZmPep3, or 5 µM Gln-18:3. (e) Corresponding newly created IBM RIL marker map of the FAC sensitivity locus. (f) The relative location of 19 genes present in the refined FAC sensitivity locus with the LRR-RLK marked as a black arrow. Coordinates and gene numbers are based on the B73 RefGen_V4 annotations. Student *t*-tests (two-tailed distribution, unpaired) were used for the detection of significant differences. Asterisks indicate significant differences with $P < 0.05$. ns, not significant.

transcript accumulation significantly increases approximately 2-fold in rice seedlings in response to treatment with FAW OSs (Hu et al., 2018; Zhou et al., 2011). To understand whether ZmFACS is differentially expressed in maize upon FAC treatment, leaves of B73 and Mo17 plants were treated with water or Gln-18:3 and harvested after 0.5 and 1 h. In B73, but not Mo17, *ZmFACS* transcripts displayed a significant 2-fold increase in accumulation 1 h after Gln-18:3 treatment (Figure 7b). Importantly, basal B73 *ZmFACS* expression levels are approximately 200-fold higher compared to Mo17 *ZmFACS* levels over the analyzed treatments and time points (Figure 7b). Given the differences in *ZmFACS* expression between the two inbred lines, genome sequences upstream and downstream of ZmFACS were compared. Comparison of the *ZmFACS* promoter sequences between B73 and Mo17 revealed large non-aligned regions, insertions of transposable element (TE) fragments in the DNA9 and Harbinger families, and an expansion of hAT TE fragments (Figure 7c) (Kohany et al., 2006). In an effort to predict the existence of aa sequence

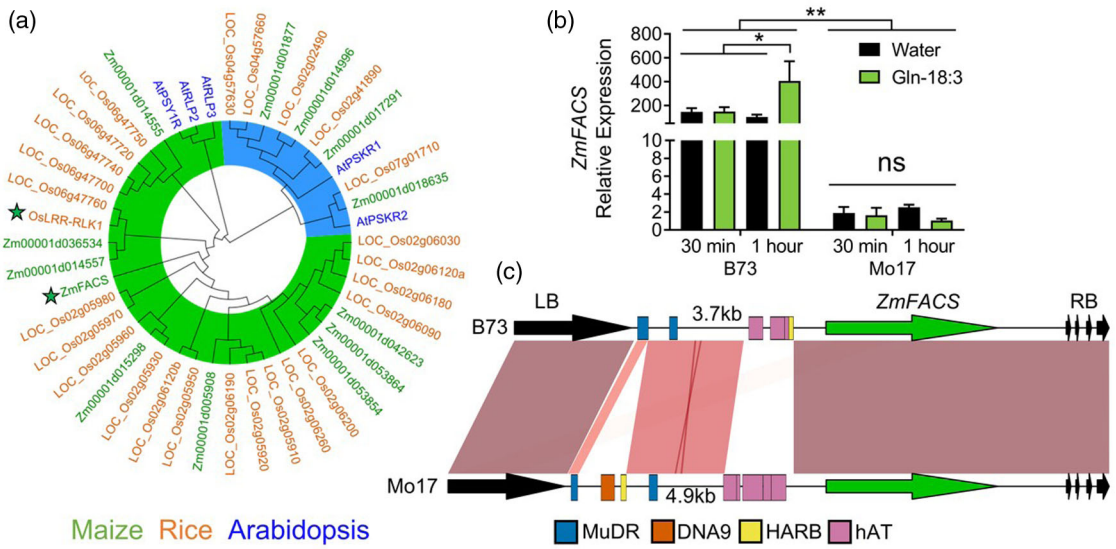

Figure 7. The candidate gene within the FAC sensitivity locus, denoted *ZmFACS*, is an ortholog of *Oryza sativa OsLRR-RLK1*, which is necessary for antiherbivore responses. (a) Phylogenetic tree generated from the protein sequences of genes related to *ZmFACS* and *OsLRR-RLK1* from *Arabidopsis thaliana* (blue font), *Oryza sativa* (orange font), and *Zea mays* (green font). Based on similarity to the *A. thaliana* genes, the phylogeny tree reveals two clades of *AtPSKR1/2*-related genes (highlighted in blue) and *AtPSY1R*-related genes (highlighted in green). ZmFACS and OsLRR-RLK1 proteins are designated by a green star. (b) Average (n = 3, +SEM) relative expression of *ZmFACS* in leaf 5 of the maize B73 and Mo17 inbred lines treated with water or Gln-18:3 for 0.5 and 1 h as determined by qRT-PCR in comparison with the expression of the control gene *Rpl17*. (c) Comparative promoter sequence similarity visualization of *ZmFACS* (blue arrows) in B73 and Mo17 including the neighboring genes upstream (LB, left border) and downstream (RB, right border) from *ZmFACS* for reference. The 3.7-kb and 4.9-kb sequences represent the genomic distance between the *ZmFACS* start codon and the LB stop codon and were used for transposable element prediction using the Poaceae Repbase database to identify a number of transposable element fragments from the MuDR family (blue), DNA9 (orange), Harbinger (HARB; yellow), and hAT (purple) families. Student *t*-tests (two-tailed distribution, unpaired) were used for the detection of significant differences. Asterisks indicate significant differences with $P < 0.05$. ns, not significant.

differences potentially disrupting function, the aligned aa sequences of B73 ZmFACS and Mo17 ZmFACS were annotated through the identification of the signal peptides, LRRs, island domain, transmembrane domain, ATP binding site, and serine/threonine protein kinase active site (Figure S3) (Casas et al., 2016; Chen, 2021; Kall et al., 2007; Mitchell et al., 2019; Sievers et al., 2011; Wang et al., 2015; Zhang et al., 2020). Of the 13 total aa differences identified, none resulted in changes predicted to have large-scale impacts on protein function (Figure S3). A comparative genomic approach was also used to search for an association between FAC insensitivity and the promoter and coding sequences (CDSs) of ZmFACS in the 27 maize inbred lines assayed. Using predicted aa sequences of ZmFACS, phylogenic analyses demonstrated that all four FAC-insensitive and four non-responsive inbred lines were distributed evenly across the tree (Figure S4a). Specifically, Mo17 ZmFACS belonged to the same clade as the FAC-responsive B73, M37W, Oh7B, and B97 ZmFACS sequences, suggesting that large-scale sequence similarity is not associated with FAC insensitivity. Comparison of the ZmFACS promoters and predicted TEs revealed a large diversity of promoter size and inserted TE families across the maize inbred lines, with no clear association to FAC insensitivity (Figure S4b). However, Mo17 ZmFACS has low transcript expression (Figure 7b) and also contains a unique combination of inserted DNA9, Harbinger, and hAT TEs (Figure S4b, Table S10) (Kohany et al., 2006). Specifically, the sole presence of a DNA9 TE in the Mo17 ZmFACS promoter sequence exists as a candidate marker that could be screened for in diverse maize germplasms in effort to test for the existence of related examples of FAC insensitivity and links to causality. From these analyses, promoter sequence variation in Mo17 *ZmFACS* and dramatically reduced transcript abundance (Figure 7b) have greater potential to represent causal differences than the comparatively modest levels of observed aa variation in the predicted ZmFACS proteins (Figure S3; Figure S4a,b; Table S10).

Heterologous expression of ZmFACS proteins enhances sensitivity to Gln-18:3 in tobacco (*Nicotiana benthamiana*)

To empirically examine if *ZmFACS* can promote FAC-elicited response sensitivity, *N. benthamiana* leaves were used as a heterologous protein expression system. As shown previously, multiple solanaceous species, including *N. benthamiana*, are naturally sensitive to FACs and activate antiherbivore defense responses upon FAC treatment (Grissett et al., 2020; Xu et al., 2015). Using ET emission to assess FAC-elicited responses, *N. benthamiana* leaves were

infiltrated with *Agrobacterium tumefaciens* carrying constructs for the C-terminal yellow fluorescent protein (YFP)-tagged fusions of ZmFACS (ZmFACS-YFP) and similarly tagged *Arabidopsis thaliana* ELONGATION FACTOR-TU RECEPTOR (AtEFR-YFP) as a control (Zipfel et al., 2006). Two days after infiltration the plants were treated with water, 1 μM elf18, or 1 μM Gln-18:3, and ET emission was measured after 2 h. Treatment of *N. benthamiana* leaves with elf18 triggered a significant increase in ET production following the expression of AtEFR-YFP but not ZmFACS-YFP (Figure S5a). In contrast, treatment with Gln-18:3 triggered significant increases in ET emission in both AtEFR-YFP- and ZmFACS-YFP- expressing leaves (Figure S5a). A positive Gln-18:3 result was anticipated given established FAC-elicited responses in *N. benthamiana* (Grissett et al., 2020). In an effort to leverage the experimental advantages of *N. benthamiana* as a rapid transient heterologous expression system, we considered alternative plant growth conditions that included lower light levels. In contrast to plants grown under normal light levels, ZmFACS-YFP-expressing plants grown under diminished light intensity selectively triggered significant ET emission following Gln-18:3 treatment (Figure S5b). We speculate that undescribed native *N. benthamiana* protein(s) mediating FAC sensitivity present under normal light conditions have reduced function in control plants (i.e., AtEFR-YFP expression) grown under diminished light. Protein levels of AtEFR-YFP and ZmFACS-YFP were probed and visualized by Western blotting, demonstrating successful heterologous expression of both (Figure S5c). Our results are consistent with ZmFACS-YFP heterologous expression increasing *N. benthamiana* responsiveness to FACs (Figure S5b). To understand the causal basis of the Gln:18:3-elicited VOC association analysis result, *N. benthamiana* plants grown under diminished light intensity were used to compare Gln-18:3 responsiveness to both B73 ZmFACS and Mo17 ZmFACS following heterologous expression. As a control, elf18 treatment triggered a significant increase in ET emission only in AtEFR-YFP-expressing leaves (Figure 8a). Likewise, only treatments with Gln-18:3 elicited significant ET emission in B73 ZmFACS-YFP- and Mo17 ZmFACS-YFP-expressing leaves (Figure 8a). Our results are consistent with the hypothesis that ZmFACS proteins from both B73 and Mo17 are functionally capable of increasing FAC response sensitivity in *N. benthamiana* (Figure 8a). Protein levels of AtEFR-YFP, B73 ZmFACS-YFP, and Mo17 ZmFACS-YFP were probed and visualized by western blotting, displaying readily detectable levels of heterologous expression (Figure 8b).

DISCUSSION

Plants respond to a complex series of exogenous cues and endogenous signals during herbivory that include HAMPs, wound-induced JAs, DAMPs, and complex amplification signals which collectively activate regulatory mechanisms promoting protective antiherbivore defenses (Erb and Reymond, 2019). For over 30 years maize has been a model system for the study of induced plant responses elicited by insect herbivory, crude insect OSs, and biochemically defined HAMPs present in insect OSs (Alborn et al., 1997; Pare et al., 1998; Turlings et al., 1990, 1993). Subsequent efforts have expanded to an array of plant–insect models; however, while diverse FAC family HAMPs are known to commonly active plant defenses, core components involving FAC-mediated signal transduction still remain undefined (Bonaventure et al., 2011; Erb and Reymond, 2019; Halitschke et al., 2001; Schmelz et al., 2009; Wu and Baldwin, 2009). Previous research has revealed that like FACs, ZmPeps potently activate classical direct and indirect antiherbivore defenses in maize (Alborn et al., 1997; Huffaker et al., 2013; Poretsky et al., 2020). The defensive biochemical outputs triggered by ZmPeps and FACs are increasingly well characterized; however, gene candidates for proximal

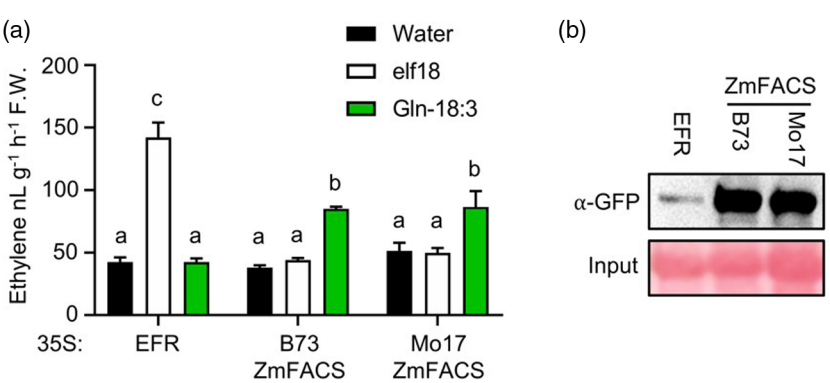

Figure 8. Transient heterologous expression in tobacco (*Nicotiana benthamiana)* of both B73 and Mo17 ZmFACS increases plant responsiveness to Gln-18:3 elicitation. (a) Average (n = 4, +SEM) elicited ethylene emission 2 h following treatment with water, 1 μM elf18, or 1 μM Gln-18:3 in *N. benthamiana* leaves expressing YFP fusion proteins with *Arabidopsis thaliana* EFR (control), B73 ZmFACS, and Mo17 ZmFACS. (b) Detection of EFR and ZmFACS cloned from B73 and Mo17 with α-GFP using Western blot. Analysis of variance, $P < 0.05$; Tukey honestly significant difference (HSD) tests, $\alpha = 0.05$; different letters (a–c) represent significant differences.

mechanisms by which FAC outputs are activated remain less clear (Gilardoni et al., 2011; Schmelz, 2015; Truitt et al., 2004). Transcriptome analyses following biotic stress and treatments with defined elicitors provide increasingly comprehensive insights into the genetic regulation of plant physiological processes (Gilardoni et al., 2010; Heidel and Baldwin, 2004; Poretsky et al., 2020; Tzin et al., 2015, 2017; Zhou et al., 2011). In the context of microbial pathogens, characterization of transcriptional reprogramming following treatment with diverse defense elicitors led to the identification of a shared core of Arabidopsis immune response genes and highlighted conserved roles for glutamate receptor-like calcium-permeable channels in general stress responses (Bjornson et al., 2021). In rice, transcriptional profiling following infestation with the caterpillar *Chilo suppressalis* led to the identification of WRKY and LRR-RLK genes involved in herbivore resistance (Hu et al., 2015, 2018). To define candidate maize regulatory genes and explore the degree of overlap between HAMP and DAMP signaling pathways, we employed both comparative transcriptional profiling and forward genetic analyses to consider genes underlying variation in plant responses to Gln-18:3 and ZmPep3.

Our comparative analyses of early-elicited transcriptional changes revealed a core set of 312 DEGs common to defined HAMP and DAMP immune responses (Figure 1, Figure 2; Table S2). Gene expression changes at 2 h revealed significant quantitative differences yet a high degree of qualitative similarity between Gln-18:3 and ZmPep3 responses. While ZmPep3 treatment resulted in >4-fold more DEGs than Gln-18:3, over 92% of positively regulated transcripts elicited by Gln-18:3 were shared by positive ZmPep3 responses (Figure S1; Table S2). Moreover, 95% of the genes that were differentially regulated by ZmPep3 displayed greater average levels in Gln-18:3-treated samples compared to the water-treated controls (Table S5). Collectively our results support a high degree of overlap between ZmPep3- and Gln-18:3-mediated transcriptional responses in maize. From the shared DEGs, diverse regulators of ZmPep3- and Gln-18:3-induced maize responses have been identified that predominate in categories associated with signal transduction and transcriptional reprogramming (Figure 2). A core set of 44 TF genes rapidly responded to ZmPep3 and Gln-18:3, including those in WRKY, TIFY, bHLH, MYB, ERF, and DREB families (Table S6, Figure 1c). While core TFs in the bHLH and WRKY families have demonstrated roles during herbivory (Hu et al., 2015; Li et al., 2015; Schweizer et al., 2013), clearly a large array of TFs underlie extensive transcriptional changes in defense proteins and specialized metabolites following herbivory (Erb and Reymond, 2019; Poretsky et al., 2020; Tzin et al., 2017). Within TF families, the greatest DAMP-associated DEG enrichment was observed in the TIFY family (Figure 2; Table S6), which have established roles in the regulation of JA signaling (Chung and Howe, 2009). A classical feature of Gln-18:3 and ZmPep3 elicitation in maize is the rapid accumulation of JAs that occurs 2 h after treatment (Huffaker et al., 2013; Schmelz et al., 2003). Family enrichment and elevated TIFY expression is consistent with strongly activated JA signaling mediated by ZmPep3 and Gln-18:3 (Erb and Reymond, 2019; Poretsky et al., 2020). Additionally, the expression of genes encoding numerous RLKs/RLPs/lectin receptors, MAPK/MAP2K/MAP3K, and CDPKs were elevated, indicating specific networks likely to participate in phosphorylation cascades controlling response outputs (Figure 2; Table S6). Transcripts for several maize orthologs of Arabidopsis genes encoding core components of wound and ROS-mediated signaling pathways, for example nicotinamide adenine dinucleotide phosphate (NADPH) oxidase family members termed RBOHs and GLRs, also accumulated (Mousavi et al., 2013; Torres et al., 2002). Many of these transcriptionally regulated candidate genes are similar to genes mediating antiherbivore defense signaling in other species (Arimura et al., 2005; Howe and Jander, 2008; Maffei et al., 2007a, 2007b). Our transcriptomic study pinpoints discrete members within maize gene families for further characterization as predicted regulators of antiherbivore defense responses. These results also suggest that while ZmPep3 is a more potent elicitor in maize, Gln-18:3 and ZmPep3 share highly similar signaling components for antiherbivore response activation. Given the observed HAMP and DAMP overlap, the 1692 significant DEGs observed following ZmPep3 treatment provide a comprehensive view of early defense-related changes at the transcriptome level. While a useful starting point, it would be unreasonable to predict that all genes of interest surrounding HAMP signaling will display significant transcriptional changes following elicitation at any one time point. Many candidate genes could potentially represent new nodes in either HAMP or DAMP signaling yet are not readily captured by transcriptomic data alone (Dressano et al., 2020).

The earliest insights into herbivore-, OS-, and HAMP-specific maize responses involved the analyses of elicited VOC production as indirect defenses (Alborn et al., 1997; Turlings et al., 1990, 1993). When measured over time, foliar sesquiterpenes dominate the late-term profiles of herbivore- and HAMP-elicited maize VOCs (Schmelz et al., 2003; Turlings et al., 1998). Using both ZmPep3- and Gln-18:3-induced production of volatile sesquiterpenes, we screened for genetic variation in diverse maize inbred lines and found that a majority produced significant responses to both elicitors (Figure 3). Four inbred lines, namely Ky21, HP301, Ms71, and CML333, did not exhibit statistically significant increases in sesquiterpene emission in response to either treatment. Our results were generally consistent with a previous study observing low terpene emission in these same lines upon elicitation with the synthetic

6-substituted indanoyl isoleucine conjugate analog of JA-isoleucine (Richter et al., 2016). The low VOC response to three different elicitors is either consistent with impaired defense signaling common to all three or alternatively suggests that elicited protective responses in these lines rely predominantly on non-volatile defenses. Our study failed to detect a single inbred line responsive to Gln-18:3 yet specifically non-responsive to ZmPep3. Collectively this supports the possible existence of defined maize inbred lines, such as Ky21, with compromised signaling in shared pathways downstream of HAMPs, DAMPs, and JAs (Figure 3b) (Richter et al., 2016). This is intriguing as many core signaling pathways are governed by gene family duplications and redundancies that create resiliency to single null mutations. For example, analyses of ZmPep receptor mutants, *Zmpepr1* and *Zmpepr2*, demonstrated that ZmPeps signal through both receptors (Poretsky et al., 2020). Genetic redundancy displayed for both *ZmPROPEP* genes and *ZmPEPR* receptors is consistent with the known role of Peps/PEPRs across diverse plant species as core amplifiers of signaling elicited by multiple inputs (Huffaker et al., 2006; Liu et al., 2013; Poretsky et al., 2020; Ross et al., 2014; Shinya et al., 2016; Tintor et al., 2013; Yamaguchi et al., 2010). In contrast, several maize inbred lines were found to be specifically insensitive to Gln-18:3 as assigned by the elicited sesquiterpene volatile production assays (Figure 3c). A reanalysis of Mo17 further demonstrated a selective deficiency to elicited ET production following Gln-18:3 treatment yet robust production after ZmPep3 treatment (Figure 4b). Given that HAMP-elicited ET emission commonly occurs rapidly after elicitation and precedes significant VOC emission (von Dahl et al., 2007; Schmelz et al., 2007), we classified Mo17 as compromised in an early signaling node specifically acting downstream of Gln-18:3. A parallel forward genetics approach was then focused on narrowing the selection of candidate genes influencing HAMP signaling in maize.

To interpret selective plant responses, we used dual-input association analyses to ensure that the specific insensitivity of Mo17 to Gln-18:3 could be assessed in each IBM RIL line compared to positive ZmPep3 responses. Using the fold change in total elicited volatiles as a mapping trait, a single locus on chromosome 4 was identified to be significantly associated with sensitivity to Gln-18:3, but not to ZmPep3 (Figure 4c). Further association analyses using individual volatile traits derived from different biosynthetic pathways demonstrated that Gln-18:3-induced production mapped to the same locus in each case and supported the hypothesis that the underlying genetic difference was likely to affect signaling pathways rather than core VOC biosynthetic capacities (Figure S2a–f). Following multiple NIL- and RIL-based fine-mapping approaches, enabled by comprehensive B73 and Mo17 community resources, we narrowed the FAC sensitivity locus to 19 genes (Figures 5 and 6). At the physical center of the locus we identified the LRR-RLK signaling candidate gene *ZmFACS* (Figure 6f). Surprisingly, *ZmFACS* is a member of the *PSY1* receptor family, which also includes the rice gene *OsLRR-RLK1* that was recently demonstrated to contribute to antiherbivore defenses (Hu et al., 2018) (Figure 7a). Transcript analyses demonstrated that expression of *OsLRR-RLK1* was induced in rice during sustained striped stemborer (SSB, *Chilo suppresalis*) herbivory as well as following FAW OS application. Gene silencing of *OsLRR-RLK1* resulted in rice plants displaying diminished JA and ET production and decreased MAPK3/6 activation following SSB infestation (Hu et al., 2018). SSB-induced increases in expression of several rice WRKY TF genes were delayed in *OsLRR-RLK1*-silenced plants and reduced production of defensive trypsin inhibitors coincided with decreased SSB resistance. In contrast, upon mechanical wounding alone *OsLRR-RLK1*-silenced plants demonstrated no difference from wild-type controls in JA/ET production, MAPK activation, or defense gene expression (Hu et al., 2018). A recently presented hypothesis postulates that *OsLRR-RLK1* is specifically involved in regulating these outputs in response to an unknown family of HAMPs which are not present during simple mechanical damage (Hu et al., 2018). In the current effort, we employed multiple forward genetics approaches to identify *ZmFACS* as a gene candidate linked to maize insensitivity to a biochemically defined HAMP, specifically Gln-18:3 (Pare et al., 1998; Truitt et al., 2004). Given the diverse approaches employed and convergent results obtained, it is likely that ZmFACS and OsLRR-RLK1 have similar roles in transduction and propagation of specific HAMPs.

Precisely how ZmFACS mediates maize response sensitivity to Gln-18:3 remains to be demonstrated. Heterologous expression of ZmFACS in *N. benthamiana* can enhance elicited ET emission after Gln-18:3 application, supporting a role in promoting FAC responses (Figure 8a). In dicot models, the Arabidopsis homologs of ZmFACS and OsLRR-RLK1, AtPSKR1 and AtPSY1R, have been implicated in regulating pathogen resistance and wound responsiveness through upregulation of JA signaling in addition to their canonical role as PSK and PSY1 receptors, respectively (Igarashi et al., 2012; Mosher and Kemmerling, 2013; Mosher et al., 2013; Shen and Diener, 2013). Receptors may mediate signaling through direct ligand binding or through activating or repressing pathway functions (Han et al., 2014; Hohmann et al., 2017; Smakowska-Luzan et al., 2018). In a legume model for plant–herbivore interactions, cowpea (*Vigna unguiculata*) was recently leveraged in forward genetic mapping approaches using the inceptin family HAMP peptides to uncover the LRR-RLP inceptin receptor (INR) (Steinbrenner et al., 2020). Physical interactions between inceptin, INR, and members of the somatic embryogenesis receptor kinase (SERK) family co-receptor

associations were supported by labeled ligand binding assays. Importantly stable heterologous expression of INR in tobacco plants conferred both inceptin-induced responses and enhanced *Spodoptera* resistance (Steinbrenner et al., 2020). Diverse receptors are increasingly implicated in regulating antiherbivore responses in multiple species through a variety of mechanisms. Reverse genetic approaches were used to partly characterize receptors from tobacco (*Nicotiana attenuata*) and rice (*O. sativa*) that regulate antiherbivore responses. The *N. attenuata* co-receptor NaSERK3/BAK1 was examined due to established roles for Arabidopsis orthologs in flagellin signaling, and when silenced, resulted in reduced wound- and OS-induced JA accumulation, but not reduced MPK activity or herbivore resistance, suggesting that NaBAK1 acts downstream of OS perception (Yang et al., 2011). Because NaSERK1 was not silenced, it is possible that the wound- and OS-induced MPK activation were not reduced due to the presence of redundant SERK co-receptors and that full activation of induced antiherbivore responses requires both NaSERK1 and NaSERK3 (Ma et al., 2016; Yang et al., 2011). Herbivore Danger Signal (HDS)-ASSOCIATED RLK1 (HAK1) and HAK2 were identified through a sequence-mining approach to identify receptors transcriptionally responsive to fractionated *Spodoptera litura* OSs enriched in polysaccharides based on sequence homology to CERK receptors involved in recognition of chitin polysaccharides (Uemura et al., 2020). Arabidopsis *hak1* insertional knockout lines demonstrated reduced responses to an OS fraction containing polysaccharides, with the receptor-like cytoplasmic kinase (RLP) PBL27 identified as a HAK1-interacting coregulator (Uemura et al., 2020). Similarly, the *N. attenuata* receptor gene *LECTIN RECEPTOR KINASE1* (NaLRK1) was among the most highly transcriptionally upregulated genes following FAC treatment (Gilardoni et al., 2010; Zhou et al., 2011). Silencing of *NaLRK1* resulted in reduced accumulation of SA, but not JA, after OS treatment, suggesting a role in regulating a subset of responses downstream of OS perception (Gilardoni et al., 2011).

Like many receptors previously identified as candidate regulators of antiherbivore defense responses, the precise molecular mechanism by which ZmFACS mediates sensitivity to Gln-18:3 remains to be determined. While heterologous expression of ZmFACS in *N. benthamiana* enhances response sensitivity to Gln-18:3, additional experiments are required to determine if ZmFACS is necessary or sufficient for FAC sensitivity in maize. ZmFACS knockdown or defined CRISPR/Cas9 *Zmfacs* mutants must be generated in B73 to fully prove that ZmFACS is required for FAC-elicited defense responses. Stable heterologous expression of FACS in non-responding plant species could be accomplished to determine if the gene is sufficient to confer sensitivity to Gln-18:3. While FACs have not yet been identified as a component of *C. suppressalis* OSs, FAC family HAMPs occur in the OSs of at least 19 examined lepidoptera species (Yoshinaga et al., 2010). Thus, comparative testing of FAC sensitivity in *OsLRR-RLK1*-silenced rice lines could be informative. More broadly, the evaluation of comparative defense responses after FAC treatment and a range of different elicitors, such as Peps or chitin, could further inform whether *OsLRR-RLK1* might selectively function in FAC signaling. In addition to these studies, experiments assessing whether ZmFACS directly binds Gln-18:3 as a ligand are of interest. Evidence for the existence of an FAC-binding protein was demonstrated using enriched plasma membrane preparations from hybrid maize (var. Delprim) and a [^{3}H]-radiolabeled FAC (Truitt et al., 2004). A critical assessment of whether ZmFACS or OsLRR-RLK1 functions through direct interaction with FACs will prove challenging. Modern standards of proof are significant and a recent critical analysis of the entire field of research states that 'a *bona fide* HAMP/PRR pair has yet to be discovered' (Reymond, 2021). One primary challenge in determining whether Gln-18:3 might directly interact with FACS is that only modest radioisotope changes. This is broadly consistent with lipid-derived ligands that are comparatively intolerant to significant modification (Merkler and Leahy, 2018). The lack of free amide groups in Gln-18:3 makes acridinium conjugate labeling similarly unfeasible (Steinbrenner et al., 2020). Biophysical ligand binding assays could overcome this challenge (Sandoval and Santiago, 2020; Sharma and Russinova, 2018); however, within seconds of contacting the wounded leaf surface FACs undergo rapid lipoxygenase-mediated modifications, resulting in active and inactive oxygenated derivatives (VanDoorn et al., 2010). Rapid plant-mediated modification of FACs creates an open question regarding the natural receptor ligands and could complicate the use of *in vitro* binding assays that lack modifying enzymes.

Our transcriptomic analyses of early maize responses to ZmPep3 and Gln-18:3 identified a targeted set of 312 shared transcriptionally co-regulated genes rich in signaling candidates. With an independent forward genetics approach we uncovered the candidate gene *ZmFACS* associated with maize FAC sensitivity. Most conceptually related studies have relied upon combinations of transcriptional profiling, candidate gene mutation, and silencing approaches to highlight genes influencing herbivory signaling (Gilardoni et al., 2011; Hu et al., 2015; Hu et al., 2018, p.1; Uemura et al., 2020; Yang et al., 2011, p.1). Of the diverse published efforts that examine FAC-elicited plant defense responses, the current study is the first to utilize both transcriptome changes and forward genetics to identify a gene candidate mediating FAC-elicited response sensitivity. Elicitor-induced antiherbivore signaling and defense activation have long been examined given the promise to naturally limit arthropod-based crop damage, but

applications are constrained by limited mechanistic knowledge (Karban and Baldwin, 1997; Kessler and Baldwin, 2002). As a rather unique model family of HAMPs, FACs have been closely examined by diverse research groups for a quarter of a century and are established to both widely occur in lepidoptera herbivores and broadly elicit defenses responses in diverse monocot and dicot plants (Grissett et al., 2020; Halitschke et al., 2001; Schmelz et al., 2009; Shinya et al., 2016; Yoshinaga et al., 2010). Lepidoptera pests in the genus *Spodoptera* drove early discoveries of HAMP-induced plant responses mediated by FACs and informed critical concepts of complex yet common plant–insect interactions more broadly (Alborn et al., 1997; Ling et al., 2021; Turlings and Erb, 2018; Turlings et al., 1993). An improved molecular understanding of how HAMP responses mediated by FACs are activated to directly or indirectly suppress *Spodoptera* pests (Alborn et al., 1997) has the continued potential to guide the development of improved crop resistance to herbivores.

EXPERIMENTAL PROCEDURES

Plant materials and growth conditions

Maize (*Z. mays*) seeds for B73, Mo17, W22, and NAM (McMullen et al., 2009) parental line seeds and B73 × Mo17 NILs were obtained from the Maize Genetics Cooperation Stock Center (Urbana, IL, USA). Maize seeds for the IBM RILs (Lee et al., 2002) were provided by Dr. Peter Balint-Kurti (U.S. Department of Agriculture-Agricultural Research Service [USDA-ARS]). All maize lines used for association analyses are listed (Table S7). Maize plants were grown in BM2 soil (Berger Mixes, Saint-Modeste, Quebec, Canada) inside a greenhouse (12 h light, minimum of 300 μmol m^{-2} s^{-1}, and 12 h dark) under a 24°C/28°C (night/day) temperature cycle. Maize plants were supplemented with a 18-18-21 Tomato Plant Food fertilizer (Miracle-Gro) and grown for 21–25 days before use of leaves. The maize plants that were used for the combined RNA-seq and VOC analyses were grown inside a growth room (16 h light, at 150 μmol m^{-2} s^{-1}, and 8 h dark cycle) at 22°C. *Nicotiana benthamiana* plants were grown inside a growth room under two different conditions, normal light intensity (150 μmol m^{-2} s^{-1}) and reduced light intensity (80 μmol m^{-2} s^{-1}), as specified. For plants grown under reduced light intensity the light intensity was further reduced (10 μmol m^{-2} s^{-1}) by disconnecting the overhead lights on the shelf in the growth room immediately following *Agrobacterium* infiltration and until elicitor treatment 2 days later. In both normal and reduced light intensity conditions, a Gro Lite WS lamp (Interlectric Corp.) was included as a supplementary light source and the plants experienced a 16/8 h light/dark cycle at 22°C. The plants were planted in BM2 soil and supplemented with 20-20-20 General Purpose fertilizer (Jack's Professional, JR Peters, Inc., Allentown, PA).

Elicitor treatment of plant leaves

The peptides elicitors ZmPep3 and elf18 were synthesized as 23-mers and received at 95% purity (Sigma-Aldrich). The FAC *N*-linolenoyl L-glutamine (Gln-18:3) was synthesized as described (Alborn et al., 2000) and obtained as a gift from Dr. Hans Alborn (USDA-ARS). All elicitors were diluted in water to the concentrations indicated. All maize treatments were performed on leaf 5 of 3-week-old plants. For the elicitation of volatiles, excised leaves were placed into individual 4-ml vials containing 1 ml of the treatment solutions for 16 h of darkness prior to volatile collections. For RNA-seq analysis whole B73 leaves were excised and put in 4-ml vials containing 1 ml of the treatment solutions for 2 h, after which 2 inches from the base of the leaves were cut and flash frozen in liquid N_2. For the analysis of transcript abundance by quantitative real-time PCR (qRT-PCR), leaf tissue was treated by scratch application of 20 μL treatment solutions for the specified times prior to flash freezing tissue in liquid N_2. For measurement of ET production, maize leaves were excised and put in 4-ml vials containing 1 ml of treatment solution for 1 h before being inserted into a sealed 7-ml vial for 1 h of head space collection as described (Schmelz et al., 2006). Measurement of ET production in *N. benthamiana* leaves was conducted using plants grown under two distinct growth conditions, normal light intensity and diminished light intensity. For the treatments, two of the most recent fully expanded leaves of 4-week-old plants grown under normal light intensity or 5-week-old plants grown under diminished light intensity were infiltrated with *A. tumefaciens* carrying constructs for the indicated YFP fusion *LRR-RLK* genes 2 days before treatment. After 2 days the *N. benthamiana* leaves were infiltrated with the treatment solutions and three leaf disks were immediately cut with a 13-mm cork borer and sealed in a 7-ml vial for 2 h before head space ET collection.

Measurement of plant volatiles

Collection of VOCs from maize leaves was conducted by enclosing the leaves in glass tubes under light for 30 min and collecting head space volatiles on a 50 mg Porapak Q (80/100 mesh; Sigma Aldrich). VOCs were eluted using methylene chloride with the addition of nonyl acetate as an internal standard and analyzed by gas chromatography (GC) and flame ionization detection (FID) as previously described (Schmelz et al., 2001). Established *Spodoptera*-elicited maize volatiles (Turlings et al., 1991) including (*Z*)-3-hexenyl acetate, linalool, DMNT, β-caryophyllene, (*E*)-α-bergamotene, (*E*)-β-farnesene, and *E*-nerolidol were identified by comparing their retention times with those of pure standards. ET production was measured by enclosing leaves in a 7-ml tube and collecting head space volatiles for 2 h. A 1-ml sample was then analyzed by GC-FID and quantified using an ET standard curve as described (Schmelz et al., 2006).

RNA preparation and transcriptome analyses

Total RNA was isolated with the NucleoSpin RNA plant kit (Clontech), treated with the Turbo DNA-free kit (Ambion), and quantified using a Qubit 2.0 fluorometer (Life Technologies). RNA-seq data were prepared by Novogen Corporation. Briefly, insert size was checked on an Agilent 2100 Bioanalyzer (Agilent Technologies) and sequencing of the 250–300-bp insert cDNA library was conducted using an Illumina HiSeq platform PE150. RNA-seq raw reads were deposited to the NCBI Sequence Read Archive (SRA) and are available under the BioProject accession number PRJNA754421. Filtering of raw reads was done by discarding reads with adaptor contaminations, reads with more than 10% of uncertain nucleotides, and reads with more than 50% low-quality nucleotides (base quality < 20). TopHat2 was used to align reads to the Maize RefGen_V4 genome with default parameters and mismatch parameter set to 2 (Kim et al., 2013). HTSeq was used to analyze gene expression levels in union mode (Anders et al., 2015). DESeq was used for analysis of differential gene expression followed by calculation of *P*-values using the negative binomial

distribution and adjusted using the Benjamini–Hochberg procedure for the false discovery rate (FDR) (Anders and Huber, 2010). Genes with $|\log_2(\text{fold change})| > 1$ and adjusted *P*-value < 0.05 were considered differentially expressed. GO term enrichment analysis was conducted with the Phytozome GO term annotation for Maize B73 V4 using the hypergeometric test to identify enriched GO terms with Benjamini–Hochberg FDR-adjusted *P*-value < 0.05 (Goodstein et al., 2012). The Maize B73 V4 MAPMAN bin annotations were used for bin enrichment analysis using the hypergeometric test to identify bins with Benjamini–Hochberg FDR-adjusted *P*-value < 0.05 (Thimm et al., 2004).

Association mapping to identify a maize FAC sensitivity locus

To screen for the genetic variation in maize response sensitivity to FAC elicitation, we examined replicated leaves ($n = 4$) of B73, Mo17, W22, and the NAM parent founders for elicited volatile emission following treatments with water, 1 μM Gln-18:3, and 1 μM ZmPep3. ZmPep3 was used as a positive control for plant responsiveness. Mo17 was among four maize inbred lines specifically insensitive to Gln-18:3. Based on differential Gln-18:3 response sensitivity in B73 and Mo17, leaves from IBM RILs were analyzed for volatile emission after treatment with water alone, 1 μM ZmPep3, or 1 μM Gln-18:3. Fold change data for elicitor-induced VOC emission were generated for 222 IBM RILs (Table S7). Association analyses were conducted in TASSEL 5.0 (Bradbury et al., 2007) using the GLM. Genotypic data from imputed IBM RIL SNP markers (July 2012 Imputed All Zea GBS final build; www.panzea.org) were filtered for a site minimum count of 10, minor allele frequencies > 10%, and major allele frequencies < 90% to generate 165 033 final SNP markers. Significantly associated SNPs were assigned following the Bonferroni *P*-value correction procedure using a cutoff of adjusted *P*-value < 0.05.

Generating a custom marker map based on SNPs called from RNA-seq data of 105 IBM RILs

Raw FASTQ files for B73, Mo17, and 105 IBM RILs were obtained from the NCBI (https://www.ncbi.nlm.nih.gov/sra) PRJNA179160 study accessions (Li et al., 2013). The raw FASTQ files were first filtered using FASTP with default parameters (Chen et al., 2018) and then aligned to the *Z. mays* B73 RegGen_4 genome obtained from plant ensemble version 44 using the STAR RNA-seq aligner with adjusted parameters (outFilterMultimapNmax 10, outFilterMismatchNoverLmax 0.04, outFilterIntronMotifs RemoveNoncanonicalUnannotated, alignIntronMax 6000) (Dobin et al., 2013). The BCFTools mpileup and call functions were used for SNP calling in all annotated CDS gene regions using the filtering parameters of DP ≥ 10 and QUAL = 999 (Li, 2011). After SNPs were called, SNPs that had more than 10 lines with an allele read depth lower than 10 were removed. A final filtering step was conducted by removing all SNPs that disagreed with the SNPs called using the control B73 and the Mo17 inbred RNA-seq reference samples. Individual SNPs were assigned gene IDs based on their location and the genotypes of genes with the associated SNPs were called based on aggregated most common SNP genotype in each gene. The genotypes of 10 043 gene-based markers were called by aggregating all the SNPs in each gene and selecting the most common allele.

RNA isolation and measurement of transcript abundance by qRT-PCR

Total RNA was isolated with TRIzol (Invitrogen) as per the manufacturer's protocol and treated with DNase according to the instructions (Life Technologies). M-MLV Reverse Transcriptase (Thermo Fisher Scientific) was used for cDNA synthesis with random decamer primers and 1 μg of RNA. For the qRT-PCR, 1 μl of 2-fold diluted cDNA was added using SsoAdvanced(tm) Universal SYBR(R) Green Supermix (Bio-Rad) and a StepOne™ Real-Time PCR System (Applied Biosystems). Based on the cycle threshold (Ct) value, ΔCt was calculated relative to the 60S ribosomal protein L17 gene (*RPL17*). All primer sequences used are listed in Table S11. Transcript abundance was calculated relative to its corresponding untreated control.

Plasmid construction for transient assays and immunoblotting in *Nicotiana benthamiana*

ZmFACS (*Zm00001d053867*) was amplified from genomic B73 and Mo17 DNA and inserted into the pENTR/D-TOPO vector (Invitrogen) (Table S11). Expression vectors of the corresponding *ZmFACS* entry vectors were generated through Gateway cloning into the destination vector pGWB441 to generate a C-terminal fusion with eYFP driven by the CaMV 35S promoter (Nakagawa et al., 2007). Expression vectors were transformed into *A. tumefaciens* GV3101 (pMP90). *Agrobacterium tumefaciens* carrying the expression vectors was infiltrated into *N. benthamiana* leaves at an OD_{600} of 0.8 for transient expression. For immunoblotting, 50 mg of leaf tissue was ground in liquid N_2 and homogenized in 100 μL 2 × SDS loading buffer (20% SDS was used in making the 5 × SDS loading buffer, instead of 10%) for 5 min at 95°C. Western blotting was performed with α-GFP polyclonal primary antibodies (ThermoFisher) at 1:1000 dilution and α-rabbit secondary antibodies (Sigma Aldrich) at 1:10 000 dilution. SuperSignal™ West Pico PLUS (ThermoFisher) chemiluminescent substrate was used for protein detection.

Phylogenetic tree construction and comparative promoter analysis

The Phytozome blastn tool was used to identify CDSs related to *FACS* from *Z. mays* var. B73 (RefGen_V4), *O. sativa* (v7.0), and *A. thaliana* (TAIR10) (Table S10) (Goodstein et al., 2012). Standalone blastn was used to identify *ZmFACS* CDSs from the assayed maize inbred lines obtained from MaizeGDB (NAM-1.0 for B73 and NAM parents, Mo17 CAU-1.0, W22 NRGENE-2.0) (Table S10) (Camacho et al., 2009; Hufford et al., 2021; Portwood et al., 2019). The CDSs of the putative genes were translated to aa sequences and the full sequences were aligned using MUSCLE with default parameters (Table S10) (Edgar, 2004). The best-fit model for the phylogenetic estimation was selected using ModelFinder (Kalyaanamoorthy et al., 2017). A maximum likelihood (ML) phylogenetic tree was constructed using IQ-TREE under the selected best-fit model, with 1000 bootstrap replications (Nguyen et al., 2015). The tree was visualized and annotated using FigTree (Rambaut, available at http://tree.bio.ed.ac.uk/software/figtree). For the comparative promoter analysis, standalone blastn was used to query the sequences of *ZmFACS* and the upstream (LB, left border) and downstream (RB, right border) neighboring genes across multiple maize inbred lines, where *ZmFACS* promoter sequences were defined as the region between the stop codon of LB and the start codon of *ZmFACS* (Table S10). Promoter sequences were compared using blastn (word_size 100, evalue 10), annotated for TEs using Repbase and plotted using genoPlotR (Camacho et al., 2009; Guy et al., 2010; Kohany et al., 2006).

ACKNOWLEDGMENTS

The authors are grateful to Dr. Philipp Weckwerth and Dr. Yezhang Ding for advice and discussions. This research was funded by

NSF-IOS PBI CAREER #1943591, a Hellman Foundation Fellowship, and UC San Diego Start-up funds to AH and by USDA NIFA AFRI #2018-67013-28125 (AH and EAS). EP was additionally funded by the Cell and Molecular Genetics (CMG) Training Program at the University of California, San Diego.

AUTHOR CONTRIBUTIONS

AH conceived the research plans. EP, MR, NA, EAS, and AH designed and performed experiments and analyzed the data. AS cloned maize receptor genes. KD prepared the samples for RNA-seq. EP, EAS, and AH wrote the manuscript with input from all authors. AH agrees to serve as the author responsible for contact and ensures communication.

CONFLICT OF INTEREST

The authors have no conflict of interest to declare.

DATA AVAILABILITY STATEMENT

All relevant data can be found within the manuscript and its supporting materials. Additionally, all RNA-seq raw reads were deposited to the NCBI SRA and are available under BioProject accession number PRJNA754421.

SUPPORTING INFORMATION

Additional Supporting Information may be found in the online version of this article.

Figure S1. Comparison of overlapping ZmPep3- and Gln-18:3-induced DEGs.

Figure S2. A forward genetics study using association analyses supports a shared maize Gln-18:3 sensitivity locus using elicited VOCs from three different biosynthetic pathways.

Figure S3. Alignment of the encoded amino acid ZmFACS sequences of B73 and Mo17.

Figure S4. Comparative genomic analysis of the ZmFACS protein sequence and promoter across different maize inbred lines.

Figure S5. Gln-18:3 response sensitivity in *N. benthamiana* is reduced in plants grown under diminished light intensity; however, transient heterologous expression of ZmFACS increases and restores responsiveness to Gln-18:3.

Table S1. Early HAMP and DAMP elicitor-induced transcriptome from treated B73 leaves.

Table S2. Summary of statistically significant differentially expressed genes (DEGs) following HAMP and DAMP elicitation of B73 leaves.

Table S3. Summary of elicitor-induced Gene Ontology (GO) term enrichment analysis.

Table S4. Summary of elicitor-induced MAPMAN bin enrichment analysis.

Table S5. Comparative analysis of elicitor-induced DEGs using ranked mean expression.

Table S6. List of elicitor-induced DEGs used for the preparation of Figure 2.

Table S7. Elicitor-induced VOC data used for forward genetics via association analyses with the IBM RIL mapping population.

Table S8. Summary table of the FAC sensitivity locus derived from association analyses and fine-mapping results.

Table S9. The newly generated IBM RIL genetic marker map based upon RNA-seq data.

Table S10. List of ZmFACS-related genes from *Zea mays*, *Oryza sativa*, and *Arabidopsis thaliana* used to generate Figure 7a,c and Figure S4a,b.

Table S11. List of primers used.

REFERENCES

Acevedo, F.E., Smith, P., Peiffer, M., Helms, A., Tooker, J. & Felton, G.W. (2019) Phytohormones in fall armyworm saliva modulate defense responses in plants. *Journal of Chemical Ecology*, **45**, 598–609.

Alborn, H.T., Hansen, T.V., Jones, T.H., Bennett, D.C., Tumlinson, J.H., Schmelz, E.A. *et al.* (2007) Disulfooxy fatty acids from the American bird grasshopper Schistocerca americana, elicitors of plant volatiles. *Proceedings of the National Academy of Sciences*, **104**, 12976–12981.

Alborn, H., Jones, T., Stenhagen, G. & Tumlinson, J. (2000) Identification and synthesis of volicitin and related components from beet armyworm oral secretions. *Journal of Chemical Ecology*, **26**, 203–220.

Alborn, H.T., Turlings, T.C.J., Jones, T.H., Stenhagen, G., Loughrin, J.H. & Tumlinson, J.H. (1997) An elicitor of plant volatiles from beet armyworm oral secretion. *Science*, **276**, 945–949.

Anders, S. & Huber, W. (2010) Differential Expression Analysis for Sequence Count Data. 12.

Anders, S., Pyl, P.T. & Huber, W. (2015) HTSeq–a Python framework to work with high-throughput sequencing data. *Bioinformatics*, **31**, 166–169.

Arimura, G., Kost, C. & Boland, W. (2005) Herbivore-induced, indirect plant defences. *Biochimica et Biophysica Acta*, **1734**, 91–111.

Bjornson, M., Pimprikar, P., Nürnberger, T. & Zipfel, C. (2021) The transcriptional landscape of Arabidopsis thaliana pattern-triggered immunity. *Nature Plants*. Available at: http://www.nature.com/articles/s41477-021-00874-5

Bonaventure, G., VanDoorn, A. & Baldwin, I.T. (2011) Herbivore-associated elicitors: FAC signaling and metabolism. *Trends in Plant Science*, **16**, 294–299.

Bradbury, P.J., Zhang, Z., Kroon, D.E., Casstevens, T.M., Ramdoss, Y. & Buckler, E.S. (2007) TASSEL: software for association mapping of complex traits in diverse samples. *Bioinformatics*, **23**, 2633–2635.

Camacho, C., Coulouris, G., Avagyan, V., Ma, N., Papadopoulos, J., Bealer, K. *et al.* (2009) BLAST+: architecture and applications. *BMC Bioinformatics*, **10**, 421.

Casas, M.I., Falcone-Ferreyra, M.L., Jiang, N., Mejía-Guerra, M.K., Rodríguez, E., Wilson, T. *et al.* (2016) Identification and characterization of maize *salmon silks* genes involved in insecticidal maysin biosynthesis. *The Plant Cell*, **28**, 1297–1309.

Chakraborty, S. & Newton, A.C. (2011) Climate change, plant diseases and food security: an overview: climate change and food security. *Plant Pathology*, **60**, 2–14.

Chen, S., Zhou, Y., Chen, Y. & Gu, J. (2018) fastp: an ultra-fast all-in-one FASTQ preprocessor. *Bioinformatics*, **34**, i884–i890.

Chen, T. (2021) Identification and characterization of the LRR repeats in plant LRR-RLKs. *BMC Molecular and Cell Biology*, **22**, 9.

Chen, Y., Ni, X. & Buntin, G.D. (2009) Physiological, nutritional, and biochemical bases of corn resistance to foliage-feeding fall armyworm. *Journal of Chemical Ecology*, **35**, 297–306.

Chung, H.S. & Howe, G.A. (2009) A critical role for the TIFY motif in repression of jasmonate signaling by a stabilized splice variant of the JASMONATE ZIM-domain protein JAZ10 in *Arabidopsis*. *The Plant Cell*, **21**, 131–145.

Dafoe, N.J., Thomas, J.D., Shirk, P.D., Legaspi, M.E., Vaughan, M.M., Huffaker, A. *et al.* (2013) European corn borer (Ostrinia nubilalis) induced responses enhance susceptibility in maize. *PLoS One*, **8**, e73394.

Day, R., Abrahams, P., Bateman, M., Beale, T., Clottey, V., Cock, M. *et al.* (2017) Fall armyworm: impacts and implications for Africa. *Outlooks on Pest Management*, **28**, 196–201.

Degen, T., Dillmann, C., Marion-Poll, F. & Turlings, T.C.J. (2004) High genetic variability of herbivore-induced volatile emission within a broad range of maize inbred lines. *Plant Physiology*, **135**, 1928–1938.

Diezel, C., von Dahl, C.C., Gaquerel, E. & Baldwin, I.T. (2009) Different lepidopteran elicitors account for cross-talk in herbivory-induced phytohormone signaling. *Plant Physiology*, **150**, 1576–1586.

Ding, Y., Weckwerth, P.R., Poretsky, E., Murphy, K.M., Sims, J., Saldivar, E. *et al.* (2020) Genetic elucidation of interconnected antibiotic pathways

mediating maize innate immunity. *Nature Plants*, **6**, 1375–1388. https://doi.org/10.1038/s41477-020-00787-9

Dobin, A., Davis, C.A., Schlesinger, F., Drenkow, J., Zaleski, C., Jha, S. *et al.* (2013) STAR: ultrafast universal RNA-seq aligner. *Bioinformatics*, **29**, 15–21.

Douglas, A.E. (2018) Strategies for enhanced crop resistance to insect pests. *Annual Review of Plant Biology*, **69**, 637–660.

Dressano, K., Weckwerth, P.R., Poretsky, E., Takahashi, Y., Villarreal, C., Shen, Z. *et al.* (2020) Dynamic regulation of Pep-induced immunity through post-translational control of defence transcript splicing. *Nature Plants*, **6**, 1008–1019.

Edgar, R.C. (2004) MUSCLE: a multiple sequence alignment method with reduced time and space complexity. *BMC Bioinformatics*, **5**, 113.

Eichten, S.R., Foerster, J.M., de Leon, N., Kai, Y., Yeh, C.-T., Liu, S. *et al.* (2011) B73-Mo17 near-isogenic lines demonstrate dispersed structural variation in maize. *Plant Physiology*, **156**, 1679–1690.

Engelberth, J., Alborn, H.T., Schmelz, E.A. & Tumlinson, J.H. (2004) Airborne signals prime plants against insect herbivore attack. *Proceedings of the National Academy of Sciences*, **101**, 1781–1785.

Erb, M. (2018) Plant defenses against herbivory: closing the fitness gap. *Trends in Plant Science*, **23**, 187–194.

Erb, M., Meldau, S. & Howe, G.A. (2012) Role of phytohormones in insect-specific plant reactions. *Trends in Plant Science*, **17**, 250–259.

Erb, M. & Reymond, P. (2019) Molecular interactions between plants and insect herbivores. *Annual Review of Plant Biology*, **70**, 527–557.

Erb, M., Veyrat, N., Robert, C.A.M., Xu, H., Frey, M., Ton, J. *et al.* (2015) Indole is an essential herbivore-induced volatile priming signal in maize. *Nature Communications*, **6**, 6273.

Felton, G.W. & Tumlinson, J.H. (2008) Plant–insect dialogs: complex interactions at the plant–insect interface. *Current Opinion in Plant Biology*, **11**, 457–463.

Fürstenberg-Hägg, J., Zagrobelny, M. & Bak, S. (2013) Plant Defense against Insect Herbivores. *International Journal of Molecular Sciences*, **14**, 10242–10297.

Gilardoni, P.A., Hettenhausen, C., Baldwin, I.T. & Bonaventure, G. (2011) *Nicotiana attenuata LECTIN RECEPTOR KINASE1* suppresses the insect-mediated inhibition of induced defense responses during *Manduca sexta* herbivory. *The Plant Cell*, **23**, 3512–3532.

Gilardoni, P.A., Schuck, S., Jüngling, R., Rotter, B., Baldwin, I.T. & Bonaventure, G. (2010) SuperSAGE analysis of the Nicotiana attenuata transcriptome after fatty acid-amino acid elicitation (FAC): identification of early mediators of insect responses. *BMC Plant Biology*, **10**, 66.

Goodstein, D.M., Shu, S., Howson, R., Neupane, R., Hayes, R.D., Fazo, J. *et al.* (2012) Phytozome: a comparative platform for green plant genomics. *Nucleic Acids Research*, **40**, D1178–D1186.

Gomez, S.K., Cox, M.M., Bede, J.C., Inoue, K., Alborn, H.T., Tumlinson, J.H. & Korth, K.L. (2005) Lepidopteran herbivory and oral factors induce transcripts encoding novel terpene synthases in *Medicago truncatula*. *Archives of Insect Biochemistry and Physiology: Published in Collaboration with the Entomological Society of America*, **58**(2), 114–127.

Grissett, L., Ali, A., Coble, A.-M., Logan, K., Washington, B., Mateson, A. *et al.* (2020) Survey of sensitivity to fatty acid-amino acid conjugates in the solanaceae. *Journal of Chemical Ecology*, **46**, 330–343.

Guy, L., Roat Kultima, J. & Andersson, S.G.E. (2010) genoPlotR: comparative gene and genome visualization in R. *Bioinformatics*, **26**, 2334–2335.

Halitschke, R., Schittko, U., Pohnert, G., Boland, W. & Baldwin, I.T. (2001) Molecular interactions between the specialist herbivore Manduca sexta (Lepidoptera, Sphingidae) and its natural host Nicotiana attenuata. III. Fatty acid-amino acid conjugates in herbivore oral secretions are necessary and sufficient for herbivore-specific plant responses. *Plant Physiology*, **125**, 711–717.

Han, Z., Sun, Y. & Chai, J. (2014) Structural insight into the activation of plant receptor kinases. *Current Opinion in Plant Biology*, **20**, 55–63.

Heidel, A.J. & Baldwin, I.T. (2004) Microarray analysis of salicylic acid- and jasmonic acid-signalling in responses of Nicotiana attenuata to attack by insects from multiple feeding guilds: defence responses to herbivores from multiple feeding guilds. *Plant, Cell and Environment*, **27**, 1362–1373.

Hohmann, U., Lau, K. & Hothorn, M. (2017) The structural basis of ligand perception and signal activation by receptor kinases. *Annual Review of Plant Biology*, **68**, 109–137.

Horikoshi, R.J., Bernardi, D., Bernardi, O., Malaquias, J.B., Okuma, D.M., Miraldo, L.L. *et al.* (2016) Effective dominance of resistance of Spodoptera frugiperda to Bt maize and cotton varieties: implications for resistance management. *Scientific Reports*, **6**, 34864.

Howe, G.A. & Jander, G. (2008) Plant Immunity to Insect Herbivores. *Annual Review of Plant Biology*, **59**, 41–66.

Hu, L., Ye, M., Kuai, P., Ye, M., Erb, M. & Lou, Y. (2018) OsLRR-RLK1, an early responsive leucine-rich repeat receptor-like kinase, initiates rice defense responses against a chewing herbivore. *New Phytologist*, **219**, 1097–1111.

Hu, L., Ye, M., Li, R., Zhang, T., Zhou, G., Wang, Q. *et al.* (2015) The rice transcription factor WRKY53 suppresses herbivore-induced defenses by acting as a negative feedback modulator of map kinase activity. *Plant Physiology*, **169**, 2907–2921.

Huffaker, A., Dafoe, N.J. & Schmelz, E.A. (2011) ZmPep1, an ortholog of Arabidopsis elicitor peptide 1, regulates maize innate immunity and enhances disease resistance. *Plant Physiology*, **155**, 1325–1338.

Huffaker, A., Pearce, G. & Ryan, C.A. (2006) An endogenous peptide signal in Arabidopsis activates components of the innate immune response. *Proceedings of the National Academy of Sciences*, **103**, 10098–10103.

Huffaker, A., Pearce, G., Veyrat, N., Erb, M., Turlings, T.C.J., Sartor, R. *et al.* (2013) Plant elicitor peptides are conserved signals regulating direct and indirect antiherbivore defense. *Proceedings of the National Academy of Sciences*, **110**, 5707–5712.

Hufford, M.B., Seetharam, A.S., Woodhouse, M.R., Chougule, K.M., Ou, S., Liu, J. *et al.* (2021) De novo assembly, annotation, and comparative analysis of 26 diverse maize genomes. *Science*, **373**, 655–662.

Igarashi, D., Tsuda, K. & Katagiri, F. (2012) The peptide growth factor, phytosulfokine, attenuates pattern-triggered immunity: attenuation of PTI by PSK. *The Plant Journal*, **71**, 194–204.

Kall, L., Krogh, A. & Sonnhammer, E.L.L. (2007) Advantages of combined transmembrane topology and signal peptide prediction–the Phobius web server. *Nucleic Acids Research*, **35**, W429–W432.

Kalyaanamoorthy, S., Minh, B.Q., Wong, T.K.F., von Haeseler, A. & Jermiin, L.S. (2017) ModelFinder: fast model selection for accurate phylogenetic estimates. *Nature Methods*, **14**, 587–589.

Karban, R. & Baldwin, I.T. (1997) *Induced Responses to Herbivory*. Chicago: University of Chicago Press.

Kessler, A. & Baldwin, I.T. (2002) Plant responses to insect herbivory: the emerging molecular analysis. *Annual Review of Plant Biology*, **53**, 299–328.

Kim, D., Pertea, G., Trapnell, C., Pimentel, H., Kelley, R. & Salzberg, S.L. (2013) TopHat2: accurate alignment of transcriptomes in the presence of insertions, deletions and gene fusions. *Genome Biology*, **14**, R36.

Kohany, O., Gentles, A.J., Hankus, L. & Jurka, J. (2006) Annotation, submission and screening of repetitive elements in Repbase: RepbaseSubmitter and Censor. *BMC Bioinformatics*, **7**, 474.

Lait, C.G., Alborn, H.T., Teal, P.E.A. & Tumlinson, J.H. (2003) Rapid biosynthesis of N-linolenoyl-L-glutamine, an elicitor of plant volatiles, by membrane-associated enzyme(s) in Manduca sexta. *Proceedings of the National Academy of Sciences*, **100**, 7027–7032.

Lee, M., Sharopova, N., Beavis, W.D., Grant, D., Katt, M., Blair, D. *et al.* (2002) Expanding the genetic map of maize with the intermated B73 × Mo17 (IBM) population. *Plant Molecular Biology*, **48**, 453–461.

Li, H. (2011) A statistical framework for SNP calling, mutation discovery, association mapping and population genetical parameter estimation from sequencing data. *Bioinformatics*, **27**, 2987–2993.

Li, L., Petsch, K., Shimizu, R., Liu, S., Xu, W.W., Ying, K. *et al.* (2013) Mendelian and non-mendelian regulation of gene expression in maize. *PLoS Genetics*, **9**, e1003202.

Li, R., Zhang, J., Li, J., Zhou, G., Wang, Q., Bian, W. *et al.* (2015) Prioritizing plant defence over growth through WRKY regulation facilitates infestation by non-target herbivores, *eLife*, **4**, e04805.

Ling, X., Gu, S., Tian, C., Guo, H., Degen, T., Turlings, T.C.J. *et al.* (2021) Differential levels of fatty acid-amino acid conjugates in the oral secretions of lepidopteran larvae account for the different profiles of volatiles. *Pest Management Science*, ps.6417.

Liu, J., Fernie, A.R. & Yan, J. (2020) The past, present, and future of maize improvement: domestication, genomics, and functional genomic routes toward crop enhancement. *Plant Communications*, **1**, 100010.

Liu, Z., Wu, Y., Yang, F., Zhang, Y., Chen, S., Xie, Q. *et al.* (2013) BIK1 interacts with PEPRs to mediate ethylene-induced immunity. *Proceedings of the National Academy of Sciences*, **110**, 6205–6210.

Ma, X., Xu, G., He, P. & Shan, L. (2016) SERKing coreceptors for receptors. *Trends in Plant Science*, **21**, 1017–1033.

Maag, D., Köhler, A., Robert, C.A.M., Frey, M., Wolfender, J.-L., Turlings, T.C.J. *et al.* (2016) Highly localized and persistent induction of *Bx1* - dependent herbivore resistance factors in maize. *The Plant Journal*, **88**, 976–991.

Maffei, M.E., Mithöfer, A. & Boland, W. (2007a) Before gene expression: early events in plant–insect interaction. *Trends in Plant Science*, **12**, 310–316.

Maffei, M.E., Mithöfer, A. & Boland, W. (2007b) Insects feeding on plants: rapid signals and responses preceding the induction of phytochemical release. *Phytochemistry*, **68**, 2946–2959.

Mattiacci, L., Dicke, M. & Posthumus, M.A. (1995) β-Glucosidase: an elicitor of herbivore-induced plant odor that attracts host-searching parasitic wasps. *Proceedings of the National Academy of Sciences of the United States of America*, **92**, 2036–2040.

McMullen, M.D., Kresovich, S., Villeda, H.S., Bradbury, P., Li, H., Sun, Q. *et al.* (2009) Genetic properties of the maize nested association mapping population. *Science*, **325**, 737–740.

Merkler, D.J. & Leahy, J.W. (2018) Binding-based proteomic profiling and the fatty acid amides. *Trends in Research*, **1**.

Mitchell, A.L., Attwood, T.K., Babbitt, P.C., Blum, M., Bork, P., Bridge, A. *et al.* (2019) InterPro in 2019: improving coverage, classification and access to protein sequence annotations. *Nucleic Acids Research*, **47**, D351–D360.

Mithöfer, A. & Boland, W. (2012) Plant defense against herbivores: chemical aspects. *Annual Review of Plant Biology*, **63**, 431–450.

Montezano, D.G., Specht, A., Sosa-Gómez, D.R., Roque-Specht, V.F., Sousa-Silva, J.C., Paula-Moraes, S.V. *et al.* (2018) Host plants of *Spodoptera frugiperda* (Lepidoptera: Noctuidae) in the Americas. *African Entomology*, **26**, 286–300.

Mori, N. & Yoshinaga, N. (2011) Function and evolutionary diversity of fatty acid amino acid conjugates in insects. *Journal of Plant Interactions*, **6**, 103–107.

Mosher, S. & Kemmerling, B. (2013) PSKR1 and PSY1R-mediated regulation of plant defense responses. *Plant Signaling and Behavior*, **8**, e24119.

Mosher, S., Seybold, H., Rodriguez, P., Stahl, M., Davies, K.A., Dayaratne, S. *et al.* (2013) The tyrosine-sulfated peptide receptors PSKR1 and PSY1R modify the immunity of Arabidopsis to biotrophic and necrotrophic pathogens in an antagonistic manner. *The Plant Journal*, **73**, 469–482.

Mousavi, S.A.R., Chauvin, A., Pascaud, F., Kellenberger, S. & Farmer, E.E. (2013) GLUTAMATE RECEPTOR-LIKE genes mediate leaf-to-leaf wound signalling. *Nature*, **500**, 422–426.

Nakagawa, T., Suzuki, T., Murata, S., Nakamura, S., Hino, T., Maeo, K. *et al.* (2007) Improved gateway binary vectors: high-performance vectors for creation of fusion constructs in transgenic analysis of plants. *Bioscience, Biotechnology, and Biochemistry*, **71**, 2095–2100.

Nguyen, L.-T., Schmidt, H.A., von Haeseler, A. & Minh, B.Q. (2015) IQ-TREE: a fast and effective stochastic algorithm for estimating maximum-likelihood phylogenies. *Molecular Biology and Evolution*, **32**, 268–274.

Oikawa, A., Ishihara, A., Tanaka, C., Mori, N., Tsuda, M. & Iwamura, H. (2004) Accumulation of HDMBOA-Glc is induced by biotic stresses prior to the release of MBOA in maize leaves. *Phytochemistry*, **65**, 2995–3001.

Onkokesung, N., Gális, I., von Dahl, C.C., Matsuoka, K., Saluz, H.-P. & Baldwin, I.T. (2010) Jasmonic acid and ethylene modulate local responses to wounding and simulated herbivory in *Nicotiana attenuata* leaves. *Plant Physiology*, **153**, 785–798.

Orozco-Cardenas, M., McGurl, B. & Ryan, C.A. (1993) Expression of an antisense prosystemin gene in tomato plants reduces resistance toward Manduca sexta larvae. *Proceedings of the National Academy of Sciences*, **90**, 8273–8276.

Orozco-Cardenas, M. & Ryan, C.A. (1999) Hydrogen peroxide is generated systemically in plant leaves by wounding and systemin via the octadecanoid pathway. *Proceedings of the National Academy of Sciences*, **96**, 6553–6557.

Overton, K., Maino, J., Day, R., Umina, P., Bett, B., Carnovale, D. *et al.* (2021) Global crop impacts, yield losses and action thresholds for fall armyworm (Spodoptera frugiperda): A review. *Crop Protection*, **145**, 105641.

Pare, P.W., Alborn, H.T. & Tumlinson, J.H. (1998) Concerted biosynthesis of an insect elicitor of plant volatiles. *Proceedings of the National Academy of Sciences*, **95**, 13971–13975.

Parra, J.R.P., Coelho, A., Cuervo-Rugno, J.B., Garcia, A.G., de Andrade Moral, R., Specht, A. *et al.* (2021) Important pest species of the *Spodoptera* complex: biology, thermal requirements and ecological zoning. *Journal of Pest Science*, April, 1–18.

Pearce, G., Strydom, D., Johnson, S. & Ryan, C.A. (1991) A polypeptide from tomato leaves induces wound-inducible proteinase inhibitor proteins. *Science*, **253**, 895–898.

Poretsky, E., Dressano, K., Weckwerth, P., Ruiz, M., Char, S.N., Shi, D. *et al.* (2020) Differential activities of maize plant elicitor peptides as mediators of immune signaling and herbivore resistance. *The Plant Journal*, **104**, 1582–1602.

Portwood, J.L., Woodhouse, M.R., Cannon, E.K., Gardiner, J.M., Harper, L.C., Schaeffer, M.L. *et al.* (2019) MaizeGDB 2018: the maize multi-genome genetics and genomics database. *Nucleic Acids Research*, **47**, D1146–D1154.

Rasmann, S., Köllner, T.G., Degenhardt, J., Hiltpold, I., Toepfer, S., Kuhlmann, U. *et al.* (2005) Recruitment of entomopathogenic nematodes by insect-damaged maize roots. *Nature*, **434**, 732–737.

Ray, S., Alves, P.C.M.S., Ahmad, I., Gaffoor, I., Acevedo, F.E., Peiffer, M. *et al.* (2016) Turnabout is fair play: herbivory-induced plant Chitinases excreted in fall armyworm frass suppress herbivore defenses in maize. *Plant Physiology*, **171**, 694–706.

Ray, S., Gaffor, I., Acevedo, F.E., Helms, A., Chuang, W.-P., Tooker, J. *et al.* (2015) Maize plants recognize herbivore-associated cues from caterpillar frass. *Journal of Chemical Ecology*, **41**, 781–792.

Reymond, P. (2021) Receptor kinases in plant responses to herbivory. *Current Opinion in Biotechnology*, **70**, 143–150.

Richter, A., Schaff, C., Zhang, Z., Lipka, A.E., Tian, F., Köllner, T.G. *et al.* (2016) Characterization of biosynthetic pathways for the production of the volatile homoterpenes DMNT and TMTT in *Zea mays*. *The Plant Cell*, **28**, 2651–2665.

Romay, M.C., Millard, M.J., Glaubitz, J.C., Peiffer, J.A., Swarts, K.L., Casstevens, T.M. *et al.* (2013) Comprehensive genotyping of the USA national maize inbred seed bank. *Genome Biology*, **14**, R55.

Ross, A., Yamada, K., Hiruma, K., Yamashita-Yamada, M., Lu, X., Takano, Y. *et al.* (2014) The Arabidopsis PEPR pathway couples local and systemic plant immunity. *EMBO Journal*, **33**, 62–75.

Sandoval, P.J. & Santiago, J. (2020) In vitro analytical approaches to study plant ligand-receptor interactions. *Plant Physiology*, **182**, 1697–1712.

Schmelz, E.A. (2015) Impacts of insect oral secretions on defoliation-induced plant defense. *Current Opinion in Insect Science*, **9**, 7–15.

Schmelz, E.A., Alborn, H.T. & Tumlinson, J.H. (2001) The influence of intact-plant and excised-leaf bioassay designs on volicitin-and jasmonic acid-induced sesquiterpene volatile release in Zea mays. *Planta*, **214**, 171–179.

Schmelz, E.A., Alborn, H.T. & Tumlinson, J.H. (2003) Synergistic interactions between volicitin, jasmonic acid and ethylene mediate insect-induced volatile emission in Zea mays. *Physiologia Plantarum*, **117**, 403–412.

Schmelz, E.A., Carroll, M.J., LeClere, S., Phipps, S.M., Meredith, J., Chourey, P.S. *et al.* (2006) Fragments of ATP synthase mediate plant perception of insect attack. *Proceedings of the National Academy of Sciences*, **103**, 8894–8899.

Schmelz, E.A., Engelberth, J., Alborn, H.T., Tumlinson, J.H. & Teal, P.E.A. (2009) Phytohormone-based activity mapping of insect herbivore-produced elicitors. *Proceedings of the National Academy of Sciences*, **106**, 653–657.

Schmelz, E.A., Kaplan, F., Huffaker, A., Dafoe, N.J., Vaughan, M.M., Ni, X. *et al.* (2011) Identity, regulation, and activity of inducible diterpenoid phytoalexins in maize. *Proceedings of the National Academy of Sciences*, **108**, 5455–5460.

Schmelz, E.A., LeClere, S., Carroll, M.J., Alborn, H.T. & Teal, P.E.A. (2007) Cowpea chloroplastic ATP synthase is the source of multiple plant defense elicitors during insect herbivory. *Plant Physiology*, **144**, 793–805.

Schweizer, F., Fernández-Calvo, P., Zander, M., Diez-Diaz, M., Fonseca, S., Glauser, G. *et al.* (2013) *Arabidopsis* basic helix-loop-helix transcription factors MYC2, MYC3, and MYC4 regulate glucosinolate biosynthesis, insect performance, and feeding behavior. *The Plant Cell*, **25**, 3117–3132.

Sharma, I. & Russinova, E. (2018) Probing plant receptor kinase functions with labeled ligands. *Plant and Cell Physiology*, **59**, 1520–1527.

Shehryar, K., Khan, R.S., Iqbal, A., Hussain, S.A., Imdad, S., Bibi, A. *et al.* (2020) Transgene stacking as effective tool for enhanced disease resistance in plants. *Molecular Biotechnology*, **62**, 1–7.

Shen, Y. & Diener, A.C. (2013) Arabidopsis thaliana RESISTANCE TO FUSARIUM OXYSPORUM 2 implicates tyrosine-sulfated peptide signaling in susceptibility and resistance to root infection. *PLoS Genetics*, **9**, e1003525.

Shinya, T., Hojo, Y., Desaki, Y., Christeller, J.T., Okada, K., Shibuya, N. *et al.* (2016) Modulation of plant defense responses to herbivores by simultaneous recognition of different herbivore-associated elicitors in rice. *Scientific Reports*, **6**, 32537.

Shinya, T., Yasuda, S., Hyodo, K., Tani, R., Hojo, Y., Fujiwara, Y. *et al.* (2018) Integration of danger peptide signals with herbivore-associated molecular pattern signaling amplifies anti-herbivore defense responses in rice. *The Plant Journal*, **94**, 626–637.

Shiu, S.-H., Karlowski, W.M., Pan, R., Tzeng, Y.-H., Mayer, K.F.X. & Li, W.-H. (2004) Comparative analysis of the receptor-like kinase family in Arabidopsis and rice. *The Plant Cell*, **16**, 1220–1234.

Sievers, F., Wilm, A., Dineen, D., Gibson, T.J., Karplus, K., Li, W. *et al.* (2011) Fast, scalable generation of high-quality protein multiple sequence alignments using Clustal Omega. *Molecular Systems Biology*, **7**, 539.

Smakowska-Luzan, E., Mott, G.A., Parys, K., Stegmann, M., Howton, T.C., Layeghifard, M. *et al.* (2018) An extracellular network of Arabidopsis leucine-rich repeat receptor kinases. *Nature*, **553**, 342–346.

Smith, W.E.C., Shivaji, R., Williams, W.P., Luthe, D.S., Sandoya, G.V., Smith, C.L. *et al.* (2012) A maize line resistant to herbivory constitutively releases (E)-β-caryophyllene. *Journal of Economic Entomology*, **105**, 120–128.

Steinbrenner, A.D., Muñoz-Amatriaín, M., Chaparro, A.F., Aguilar-Venegas, J.M., Lo, S., Okuda, S. *et al.* (2020) A receptor-like protein mediates plant immune responses to herbivore-associated molecular patterns. *Proceedings of the National Academy of Sciences of the United States of America*, 202018415.

Tanaka, K., Choi, J., Cao, Y. & Stacey, G. (2014) Extracellular ATP acts as a damage-associated molecular pattern (DAMP) signal in plants. *Frontiers in Plant Science*, **5**. https://doi.org/10.3389/fpls.2014.00446

Thaler, J.S., Farag, M.A., Paré, P.W. & Dicke, M. (2002) Jasmonate-deficient plants have reduced direct and indirect defences against herbivores: Jasmonate-deficient plants. *Ecology Letters*, **5**, 764–774.

The Gene Ontology Consortium (2019) The gene ontology resource: 20 years and still going strong. *Nucleic Acids Research*, **47**, D330–D338.

Thimm, O., Bläsing, O., Gibon, Y., Nagel, A., Meyer, S., Krüger, P. *et al.* (2004) mapman: a user-driven tool to display genomics data sets onto diagrams of metabolic pathways and other biological processes. *The Plant Journal*, **37**, 914–939.

Tian, D., Peiffer, M., Shoemaker, E., Tooker, J., Haubruge, E., Francis, F. *et al.* (2012) Salivary glucose oxidase from caterpillars mediates the induction of rapid and delayed-induced defenses in the tomato plant. *PLoS One*, **7**, e36168.

Tintor, N., Ross, A., Kanehara, K., Yamada, K., Fan, L., Kemmerling, B. *et al.* (2013) Layered pattern receptor signaling via ethylene and endogenous elicitor peptides during Arabidopsis immunity to bacterial infection. *Proceedings of the National Academy of Sciences*, **110**, 6211–6216.

Torres, M.A., Dangl, J.L. & Jones, J.D.G. (2002) Arabidopsis gp91phox homologues AtrbohD and AtrbohF are required for accumulation of reactive oxygen intermediates in the plant defense response. *Proceedings of the National Academy of Sciences*, **99**, 517–522.

Truitt, C.L., Wei, H.-X. & Paré, P.W. (2004) A plasma membrane protein from *Zea mays* binds with the herbivore elicitor volicitin. *The Plant Cell*, **16**, 523–532.

Turlings, T.C.J., Alborn, H.T., Loughrin, J.H. & Tumlinson, J.H. (2000) Volicitin, an elicitor of maize volatiles in oral secretion of spodoptera exigua: isolation and bioactivity. *Journal of Chemical Ecology*, **26**, 189–202.

Turlings, T.C.J. & Erb, M. (2018) Tritrophic interactions mediated by herbivore-induced plant volatiles: mechanisms, ecological relevance, and application potential. *Annual Review of Entomology*, **63**, 433–452.

Turlings, T.C.J., Lengwiler, U.B., Bernasconi, M.L. & Wechsler, D. (1998) Timing of induced volatile emissions in maize seedlings. *Planta*, **207**, 146–152.

Turlings, T.C.J., McCall, P.J., Alborn, H.T. & Tumlinson, J.H. (1993) An elicitor in caterpillar oral secretions that induces corn seedlings to emit chemical signals attractive to parasitic wasps. *Journal of Chemical Ecology*, **19**, 411–425.

Turlings, T.C.J., Scheepmaker, J.W.A., Vet, L.E.M., Tumlinson, J.H. & Lewis, W.J. (1990) How contact foraging experiences affect preferences for host-related odors in the larval parasitoid Cotesia marginiventris (Cresson) (Hymenoptera: Braconidae). *Journal of Chemical Ecology*, **16**, 1577–1589.

Turlings, T.C.J., Tumlinson, J.H., Heath, R.R., Proveaux, A.T. & Doolittle, R.E. (1991) Isolation and identification of allelochemicals that attract the larval parasitoid, Cotesia marginiventris (Cresson), to the microhabitat of one of its hosts. *Journal of Chemical Ecology*, **17**, 2235–2251.

Tzin, V., Fernandez-Pozo, N., Richter, A., Schmelz, E.A., Schoettner, M., Schäfer, M. *et al.* (2015) Dynamic maize responses to aphid feeding are revealed by a time series of transcriptomic and metabolomic assays. *Plant Physiology*, **169**, 1727–1743.

Tzin, V., Hojo, Y., Strickler, S.R., Bartsch, L.J., Archer, C.M., Ahern, K.R. *et al.* (2017) Rapid defense responses in maize leaves induced by Spodoptera exigua caterpillar feeding. *Journal of Experimental Botany*, **68**, 4709–4723.

Uemura, T., Hachisu, M., Desaki, Y., Ito, A., Hoshino, R., Sano, Y. *et al.* (2020) Soy and Arabidopsis receptor-like kinases respond to polysaccharide signals from Spodoptera species and mediate herbivore resistance. *Communications Biology*, **3**, 224.

VanDoorn, A., Kallenbach, M., Borquez, A.A., Baldwin, I.T. & Bonaventure, G. (2010) Rapid modification of the insect elicitor N-linolenoyl-glutamate via a lipoxygenase-mediated mechanism on Nicotiana attenuata leaves. *BMC Plant Biology*, **10**, 164.

von Dahl, C.C., Winz, R.A., Halitschke, R., Kühnemann, F., Gase, K. & Baldwin, I.T. (2007) Tuning the herbivore-induced ethylene burst: the role of transcript accumulation and ethylene perception in *Nicotiana attenuata*: *Ethylene biosynthesis during herbivory*. *The Plant Journal*, **51**, 293–307.

Waiss, A.C., Chan, B.G., Elliger, C.A., Wiseman, B.R., McMillian, W.W., Widstrom, N.W. *et al.* (1979) Maysin, a flavone glycoside from corn silks with antibiotic activity toward corn earworm. *Journal of Economic Entomology*, **72**, 256–258.

Wang, J., Li, H., Han, Z., Zhang, H., Wang, T., Lin, G. *et al.* (2015) Allosteric receptor activation by the plant peptide hormone phytosulfokine. *Nature*, **525**, 265–268.

Wang, J., Yang, M., Song, Y., Acevedo, F.E., Hoover, K., Zeng, R. *et al.* (2018a) Gut-associated bacteria of Helicoverpa zea indirectly trigger plant defenses in maize. *Journal of Chemical Ecology*, **44**, 690–699.

Wang, L., Einig, E., Almeida-Trapp, M., Albert, M., Fliegmann, J., Mithöfer, A. *et al.* (2018b) The systemin receptor SYR1 enhances resistance of tomato against herbivorous insects. *Nature Plants*, **4**, 152–156.

Wouters, F.C., Blanchette, B., Gershenzon, J. & Vassão, D.G. (2016) Plant defense and herbivore counter-defense: benzoxazinoids and insect herbivores. *Phytochemistry Reviews*, **15**, 1127–1151.

Wu, J. & Baldwin, I.T. (2009) Herbivory-induced signalling in plants: perception and action. *Plant, Cell and Environment*, **32**, 1161–1174.

Xu, S., Zhou, W., Pottinger, S. & Baldwin, I.T. (2015) Herbivore associated elicitor-induced defences are highly specific among closely related Nicotiana species. *BMC Plant Biology*, **15**, 2.

Yamaguchi, Y., Huffaker, A., Bryan, A.C., Tax, F.E. & Ryan, C.A. (2010) PEPR2 is a second receptor for the Pep1 and Pep2 peptides and contributes to defense responses in *Arabidopsis*. *The Plant Cell*, **22**, 508–522.

Yang, D.-H., Hettenhausen, C., Baldwin, I.T. & Wu, J. (2011) BAK1 regulates the accumulation of jasmonic acid and the levels of trypsin proteinase inhibitors in Nicotiana attenuata's responses to herbivory. *Journal of Experimental Botany*, **62**, 641–652.

Yoshinaga, N., Aboshi, T., Abe, H., Nishida, R., Alborn, H.T., Tumlinson, J.H. *et al.* (2008) Active role of fatty acid amino acid conjugates in nitrogen metabolism in Spodoptera litura larvae. *Proceedings of the National Academy of Sciences*, **105**, 18058–18063.

Yoshinaga, N., Aboshi, T., Ishikawa, C., Fukui, M., Shimoda, M., Nishida, R. *et al.* (2007) Fatty acid amides, previously identified in caterpillars, found in the cricket Teleogryllus taiwanemma and fruit fly drosophila melanogaster larvae. *Journal of Chemical Ecology*, **33**, 1376–1381.

Yoshinaga, N., Alborn, H.T., Nakanishi, T., Suckling, D.M., Nishida, R., Tumlinson, J.H. *et al.* (2010) Fatty acid-amino acid conjugates diversification in lepidopteran caterpillars. *Journal of Chemical Ecology*, **36**, 319–325.

Zhang, W.-X., Pan, X. & Shen, H.-B. (2020) Signal-3L 3.0: improving signal peptide prediction through combining attention deep learning with window-based scoring. *Journal of Chemical Information and Modeling*, **60**, 3679–3686.

Zhou, G., Wang, X., Yan, F., Wang, X., Li, R., Cheng, J. *et al.* (2011) Genome-wide transcriptional changes and defence-related chemical profiling of rice in response to infestation by the rice striped stem borer Chilo suppressalis. *Physiologia Plantarum*, **143**, 21–40.

Zipfel, C., Kunze, G., Chinchilla, D., Caniard, A., Jones, J.D.G., Boller, T. *et al.* (2006) Perception of the bacterial PAMP EF-Tu by the receptor EFR restricts agrobacterium-mediated transformation. *Cell*, **125**, 749–760.

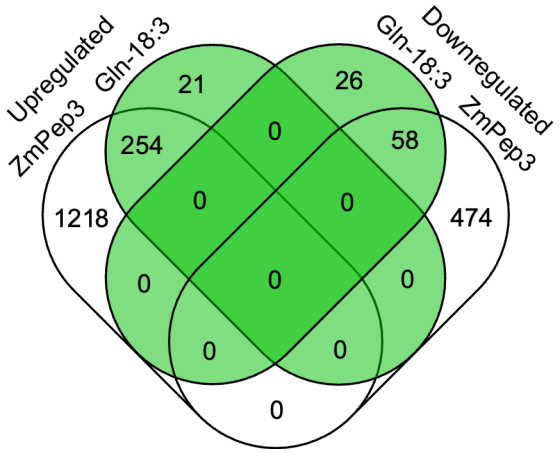

Figure S1. Comparison of overlapping ZmPep3- and Gln-18:3-induced DEGs. A venn diagram was generated to compare the upregulated and downregulated DEGs following ZmPep3 and Gln-18:3 treatments found using RNA-seq data after 2 hour treatment of maize B73 leaves. Comparison of ZmPep3- and Gln-18:3-induced DEGs revealed large scale overlap in HAMP and DAMP elicited regulation and no overlap between the upregulated and downregulated DEGs.

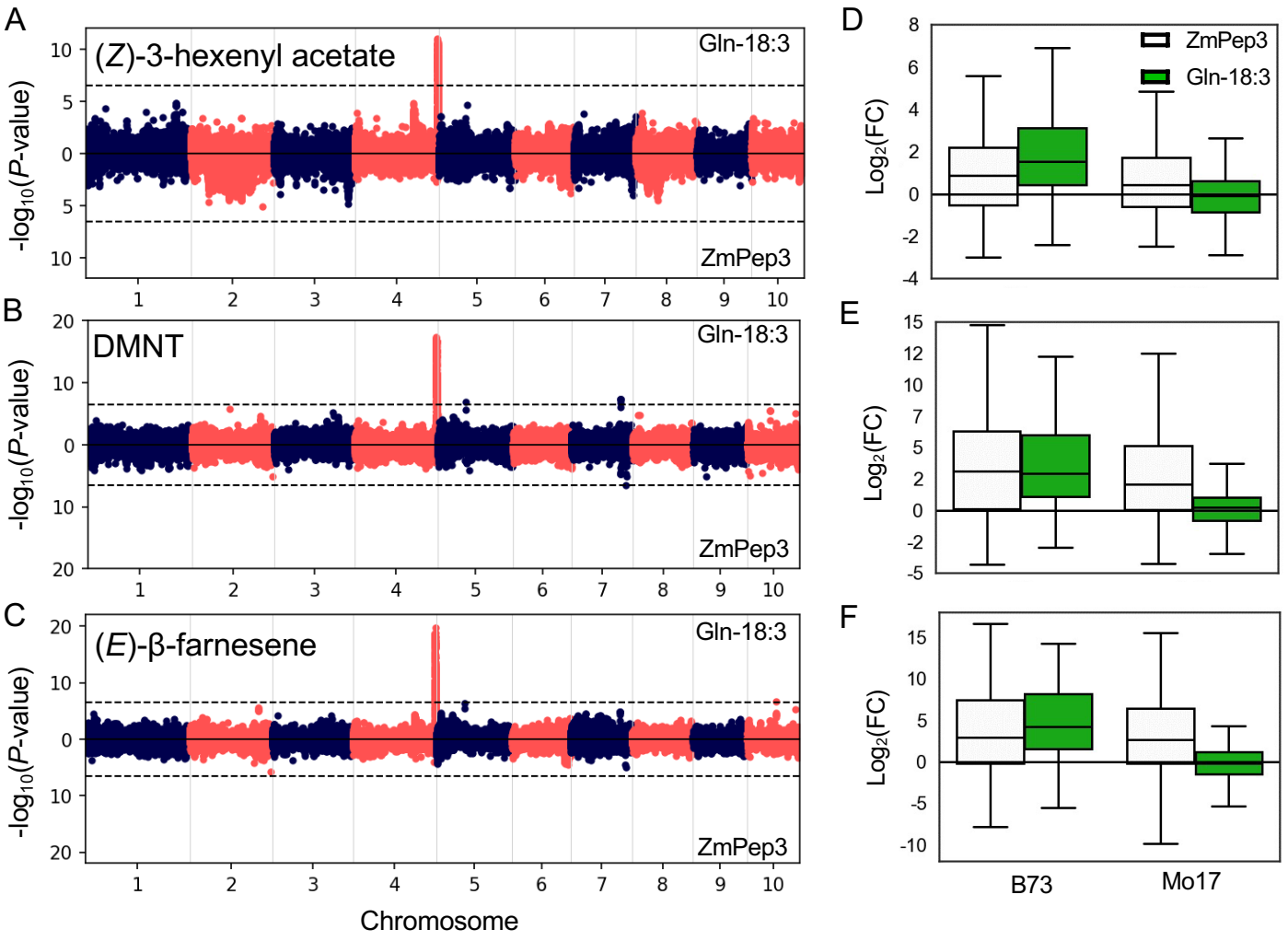

Figure S2. A forward genetics study using association analyses supports a shared maize Gln-18:3 sensitivity locus using elicited VOCs from three different biosynthetic pathways. Association analyses using imputed SNP markers (165,033) obtained from the Panzea project for the IBM RIL population and VOC fold-change values as traits derived from leaf 5 of 242 RILs treated with water, 1μM ZmPep3- and 1μM for 16 hours. Fold change (FC) values were calculated for individual elicited VOCs from different biosynthetic pathways, including **(A)** (*Z*)-3-hexenyl acetate, **(B)** (3*E*)-4,8-dimethyl-1,3,7-nonatriene (DMNT) and **(C)** (*E*)-β-farnesene. Box plots showing the distribution of elicitor-induced fold-change VOC emission for **(D)** (*Z*)-3-hexenyl acetate, **(E)** DMNT and **(F)** (*E*)-β-farnesene at the highest statistically significant SNP (B73 Ref Gen_V2; S4_237322925) associated with FAC sensitivity across the 242 IBM RILs. Dashed lines in Manhattan plots indicate significance cutoff of $P < 0.05$ based on Bonferroni correction.

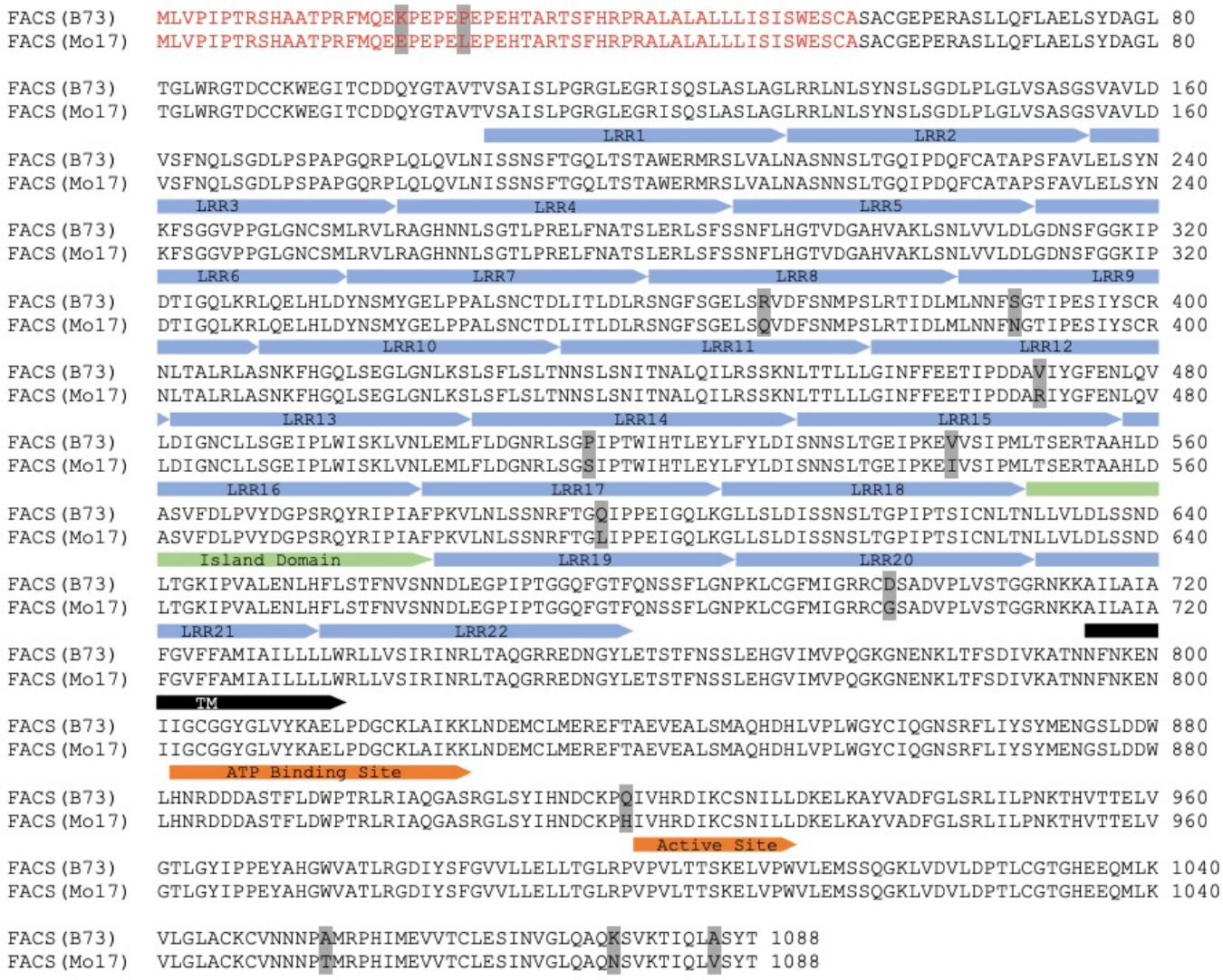

Figure S3. Alignment of the encoded amino acid ZmFACS sequences of B73 and Mo17. The amino acid sequences for B73 ZmFACS (Zm00001d053867) and Mo17 ZmFACS (Zm00014a001621) were aligned using Clustal Omega and visualized by highlighting in grey all matching amino-acids. The signal peptide, colored red, was predicted for both B73 ZmFACS and Mo17 ZmFACS using Signal-3L. The predicted LRR sequences, with a single predicted island domain between them, were manually annotated based on the consensus LRR motif sequence and labeled using a blue arrow below the matching LRR sequences. Transmembrane domain was predicted using Phobius and labeled using a black arrow below the matching sequence. Two predicted protein domains by InterPro using the amino-acid of B73 ZmFACS were included, the ATP binding site (IPR017441) and the Serine/threonine-protein kinase active site (IPR008271) and labeled using an orange arrows below the matching sequence.

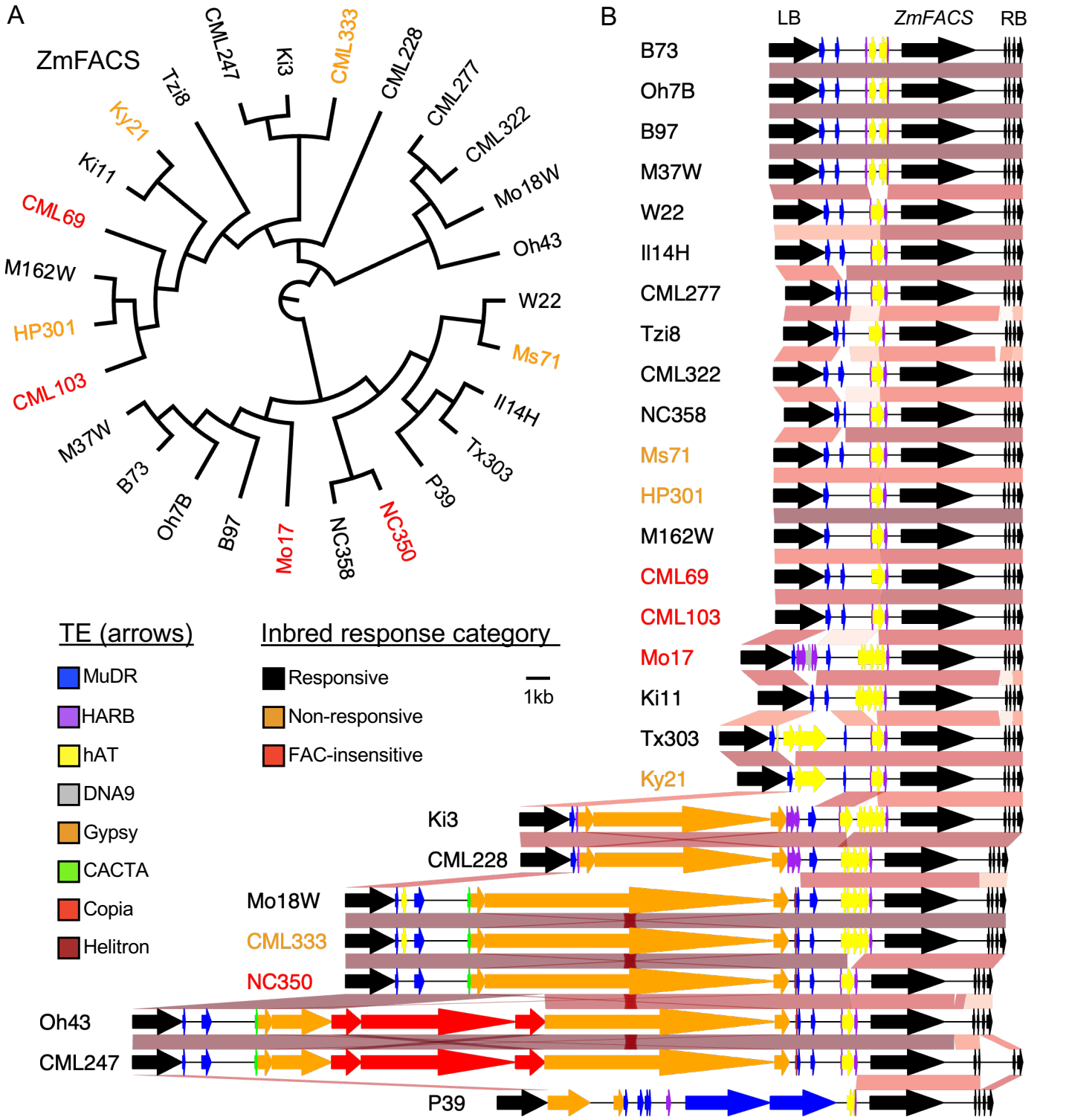

Figure S4. Comparative genomic analysis of the ZmFACS protein sequence and promoter across different maize inbreds **(A)** Phylogenetic tree generated from the protein sequences of ZmFACS from 27 maize inbreds. Responsive (black font), non-responsive (orange font) and FAC-insensitive (red font) inbreds are defined based on the results in Fig. 2. **(B)** Comparative promoter sequence similarity visualization of *ZmFACS,* including the neighboring genes upstream (LB - Left border) and downstream (RB - Right border) from *ZmFACS* for reference. The promoter regions between the *ZmFACS* start codon and the LB stop codon were used for transposable element (TE) prediction using the Poaceae Repbase database (www.girinst.org/censor) to identify TE fragments from the MuDR family, Harbinger (HARB), hAT, DNA9, Gypsy, CACTA, Copia and Helitron families, represented as differently colored arrows as defined in the legend.

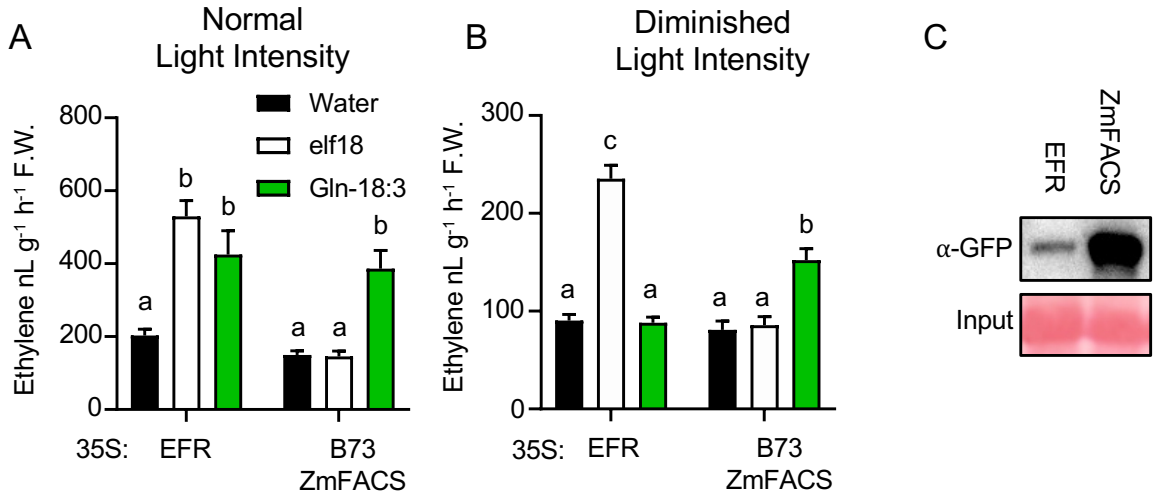

Figure S5. Native Gln-18:3 response sensitivity in *N. benthamiana* is reduced in plants grown under diminished light intensity; however, transient heterologous expression of ZmFACS increases and restores responsiveness to Gln-18:3. **(A)** Average (n=4, +SEM) ethylene emission after 2-hour treatments with either water, 1 μM elf18 or 1 μM Gln-18:3 in *N. benthamiana* leaves expressing YFP-fusion proteins with either *Arabidopsis thaliana* EFR or B73 ZmFACS. Plants were grown under normal light intensity, as described in the method section. **(B)** Average (n=4, +SEM) ethylene emission after 2-hour treatments with either water, 1 μM elf18 or 1 μM Gln-18:3 in *N. benthamiana* leaves expressing YFP-fusion proteins with either *Arabidopsis thaliana* EFR or B73 ZmFACS. Plants were grown under diminished light intensity, as described in the method section. **(C)** Detection of YFP-fusion *Arabidopsis thaliana* EFR and ZmFACS cloned from B73 using α-GFP western blot. Different letters (a, b, c) represent significant differences (All ANOVAs $P < 0.05$ followed by Tukey honestly significant difference (HSD), $\alpha = 0.05$).